THE ASTROPHYSICAL JOURNAL SUPPLEMENT SERIES, 77:417–440, 1991 November

A STANDARD STELLAR SPECTRAL SEQUENCE IN THE RED/NEAR-INFRARED: CLASSES K5 TO M9[1]

J. DAVY KIRKPATRICK, TODD J. HENRY, AND DONALD W. MCCARTHY, JR.
Department of Astronomy, Steward Observatory, University of Arizona, Tucson, AZ 85721
Received 1990 November 13; accepted 1991 April 16

ABSTRACT

Spectra of 39 K and M dwarf spectroscopic standards, as well as 38 secondary standards, are shown from 6300 to 9000 Å. This sequence of 77 spectra ranges from K5 V to M9 and has been classified on the Boeshaar system. Spectra of 14 giant and higher luminosity stars are presented from 6900 to 9000 Å, along with two miscellaneous spectra. Also given is an extensive list of atomic and molecular features found in the spectra of late K and M stars of all luminosity classes. From the spectral slopes and the strengths of the red/near-infrared spectral features it is possible to distinguish giants from dwarfs and to classify M dwarfs of all spectral subclasses. The library of spectra has been used to construct a spectral class versus mass relation which allows mass estimates to be made based upon a dwarf's spectral class alone. The relation is based on eight objects having both well-determined masses and spectral types.

Subject headings: infrared: spectra — stars: spectral classification

1. INTRODUCTION

A well-defined standard sequence for late-type stars in the red/near-infrared is useful in many astrophysical applications including spectral classification, spectral definition of subdwarf objects, calibration of the temperatures of late-type stars, definition of the end of the main sequence, detection and deconvolution of close binary systems, and development of the stellar luminosity function for the reddest stars, which is currently not well determined.

An extensive spectral catalog from classes K5–M9 is provided here. There are 77 spectra of dwarfs alone, with an additional 16 spectra of objects from other luminosity classes. For classification purposes, obtaining as large a spectral range as possible was the main priority, so the region from 6300 to 9000 Å was chosen. This region encompasses a number of titanium oxide (TiO) bands, useful in classifying early M dwarfs, and a number of vanadium oxide (VO) bands, useful in classifying late M dwarfs (see, e.g., Keenan & Schroeder 1952). The short-wavelength cutoff at 6300 Å provides overlap with the system of Boeshaar (1976), who used features out to 6800 Å and whose dwarf spectral classification system is used in this paper. The B-system band of the CaH molecule, useful as a discriminant between M dwarfs and M subdwarfs (Ake & Greenstein 1980), falls at 6385 Å, near the cutoff. The long-wavelength cutoff at 9000 Å occurs where telluric water absorption begins to dominate the spectrum. This spectral region corresponds more closely than do the bluer systems with the blackbody peaks of M dwarf stars, whose temperatures range from 4000 to 2400 K (Berriman & Reid 1987; Liebert, Boroson, & Giampapa 1984).

This large spectral range enables us to investigate whether there are any gross differences among the spectra of the latest M dwarfs which might help discriminate between two distinct groups: late-type stars and hot brown dwarfs. These spectra also provide an important link between optical and near-infrared spectra, the latter of which are quickly approaching the resolution of broad-band optical spectra used for spectral-typing purposes.

The kinds of objects chosen and the rationale behind their selection is discussed in § 2. The observation and reduction procedures for all spectroscopic data are presented in § 3. The method for classifying the spectra, using a combination of spectral features and spectral slope, is outlined in § 4, and a detailed line identification list, including over 50 features useful in describing the spectra of late-type stars, is given in § 5. The criteria used for luminosity classification, which use this line list, are discussed in § 6. In § 7, the relation between spectral class and mass for dwarf stars is presented, illustrating that mass estimates can be made for main-sequence stars based on an object's spectral class alone. The results are summarized in § 8. A justification for the late-type (M6.5 and cooler) dwarf spectral classification used in this paper is provided in Appendix A.

2. OBJECT LISTS

Primary dwarf spectral standards were taken from the lists of Boeshaar (1976), Keenan & McNeil (1976, 1989), Turnshek et al. (1985), Boeshaar & Tyson (1985), Giampapa & Liebert (1986), McCarthy et al. (1988), and Henry & Kirkpatrick (1990). All of these references use the classification system of Boeshaar (1976). Because most of the standards from Boeshaar (1976) are unobservable in the summer months, spectra of a number of M dwarfs from Gliese (1969) and other sources including Luyten (1979) were obtained and reclassified against the primary standards to generate a list of secondary standards.

The primary reason for observing giants and supergiants was to verify that these higher luminosity stars could be reliably distinguished from the dwarfs at the resolution of our data. Standards were taken from the lists of Turnshek et al. (1985),

[1] Observations reported here were obtained at the Multiple Mirror Telescope Observatory, a facility operated jointly by the Smithsonian Institution and the University of Arizona.

TABLE 1

PRIMARY DWARF SPECTRAL STANDARDS

Gliese Number	Other Name	Boeshaar Spec. Type[a]	Adopted Spec. Type	Date Obs. (UT)	Integ. (sec)
820 A	61 Cyg A	K5 V[b,c]	K5 V	1989 Jul 14	2
820 B	61 Cyg B	K7 V[b,c]	K7 V	1989 Jul 14	2
380	HD 88230	K7 V	K7 V	1990 Jan 22	5
328	BD +2°2098	M0.5 V	M0 V	1990 Jan 22	120
270	BD +33°1505	M0 V	M0 V	1990 Jan 22	597
846	HD 209290	M0.5 V	M0.5 V	1989 Jul 14	5
229	HD 42581	M1 V	M1 V	1990 Jan 22	370
205	HD 36395	M1.5 V	M1.5 V	1990 Jan 22	60
411	HD 95735	M2 V	M2 V	1990 Jan 22	9
382	BD −3°2870	M2 V	M2 V	1990 Jan 22	45
250 B	—	M2.5 V	M2.5 V	1990 Jan 22	600
381	L 968-22	M3 V	M2.5 V	1990 Jan 22	95
352 AB	BD −12°2918	M3+ V	M3 V	1990 Jan 21	8
436	BD +27°28217	M3 V	M3 V	1990 Jan 22	720
251	Wolf 294	M3.5 V	M3 V	1990 Jan 22	360
752 A	HD 180617	M3 V	M3 V	1989 Jul 10	17
725 A	HD 173739	M3 V[c]	M3 V	1989 Jul 14	5
273	BD +5°1668	M4 V	M3.5 V	1990 Jan 22	120
725 B	HD 173740	M3.5 V[c]	M3.5 V	1989 Jul 14	5
213	Ross 47	M4+ V	M4 V	1990 Jan 22	130
275.2 A	G 107-69	M4+: V	M4 V	1990 Jan 22	1200
402	Wolf 358	M4 V	M4 V	1990 Jan 22	900
83.1	L 1159-16	M4.5 V	M4.5 V	1989 Jul 24	660
268	Ross 986	M4.5 V	M4.5 V	1990 Jan 22	842
166 C	40 Eri C	M4.5 V	M4.5 V	1990 Jan 20	15
234 AB	Ross 614 AB	M4.5 V	M4.5 V	1990 Jan 22	1980
51	Wolf 47	M5 V	M5 V	1989 Jul 24	960
866 AB	L 789-6 AB	M5+ V	M5 V	1989 Jul 24	420
—	G 208-44 AB	M5+ V	M5.5 V	1989 Jul 13	75
65 A	L 726-8	M6− V[d]	M5.5 V	1990 Jan 20	25
—	G 208-45	M6 V[e]	M6 V	1989 Jul 13	225
65 B	UV Cet	M6− V[d]	M6 V	1990 Jan 20	25
406	Wolf 359	M6 V	M6 V	1990 Jan 20	80
—	LHS 523	M6.5 V[f]	M6.5 V	1989 Jul 13	600
—	G 51-15	M6.5 V	M6.5 V	1990 Jan 20	243
644 C	VB 8	M7 V[f,g]	M7 V	1989 Jul 10	1200
752 B	VB 10	M8 V[c,f,g]	M8 V	1989 Jul 10	1800
569 B	—	M8.5[h]	M8.5	1989 Jul 14	2100
—	LHS 2924	M9[f,g]	M9	1989 Jul 13	1980

[a] Boeshaar 1976 unless otherwise noted.
[b] Keenan & McNeil 1989.
[c] Turnshek et al. 1985.
[d] GL 65 A and GL 65 B typed as one spectrum by Boeshaar 1976.
[e] McCarthy et al. 1988.
[f] Giampapa & Liebert 1986.
[g] Boeshaar & Tyson 1985.
[h] Henry & Kirkpatrick 1990.

Jacoby, Hunter, & Christian (1984), and Keenan & McNeil (1976, 1989). Classification of giants presents a problem in that giants later than M5 are spectrum variables and are thus unsuitable as spectral standards (Merrill, Deutsch, & Keenan 1962; Abt 1963); the same is true of the latest supergiants although attempts at classifying both have been made (e.g., Solf 1978). No giant or supergiant stars later than M5 have been observed in this study.

M subdwarfs present a different problem. Part of the difficulty lies with the taxonomy itself, i.e., the term "subdwarf" encompasses any number of characteristics including photometric, spectral, or kinematic properties, and a star, whether it fits only one or several of these characteristics, may still be dubbed a "subdwarf." Subdwarfs include stars which are underluminous with respect to the dwarf sequence (an effect which may be due to various line or molecular blanketing effects); stars which are metal poor, indicative of an old halo (Population II) origin; and stars with velocities placing them in the halo population. For example, Barnard's Star (GL 699) is sometimes listed as a subdwarf (Veeder 1974), although its gross spectral characteristics, at least in the range covered by our data, do not distinguish it from a dwarf star. (See, however, discussions by Mould [1976] and Mould & McElroy [1978] on the use of CaH to TiO band ratios as discriminants between

TABLE 2

SECONDARY DWARF SPECTRAL STANDARDS

Gliese Number	Other Name	Published Spec. Type[a]	Adopted Spec. Type	Date Obs. (UT)	Integ. (sec)
764.1 A	HD 184860	K2 V	< K5 V	1989 Jul 14	21
250 A	HD 50281	K6 V	< K5 V	1990 Jan 22	274
340.3	HD 80632	K8 V	< K5 V	1990 Jan 22	45
775	HD 190007	K4 V	K5 V	1989 Jul 14	3
764.1 B	—	K5 V	K7 V	1989 Jul 14	21
265 A	BD +27°1311	M0 V	K7 V	1990 Jan 22	300
786	HD 193202	M0 V	K7 V	1989 Jul 14	10
748.2 A	BD +1°3942	M0 V	K7 V	1989 Jul 14	80
430	BD +63°965	M0 V	K7 V	1990 Jan 22	210
338 B[b]	HD 79210	M0 V	K7 V	1990 Jan 22	10
734 A	HD 230017	M0 V	M0 V	1989 Jul 14	15
763	HD 184489	M1 V	M0 V	1989 Jul 14	17
338 A	HD 79211	M0 V	M0 V	1990 Jan 22	10
748.2 B	G 22-21 B	—	M0 V	1989 Jul 14	80
839	G 215-20	M2 V	M0.5 V	1989 Jul 14	17
—	GJ 2155	sdM[c]	M0.5 V	1989 Jul 14	25
761.2	BD +0°4241	M1 V	M0.5 V	1989 Jul 14	35
720 A	BD +45°2743	M2 V	M0.5 V	1989 Jul 14	20
767 A	BD +31°3767	M1 V	M0.5 V	1989 Jul 14	30
220	Ross 59	M2 V	M2 V	1990 Jan 22	120
22 AC	BD +66°34	M2.5 V	M2 V	1990 Jan 21	23
806	G 209-41	M3 V	M2 V	1989 Jul 14	30
767 B	—	M2 V	M2.5 V	1989 Jul 14	30
226	AC +82°1111	M3 V	M2.5 V	1990 Jan 22	320
22 B	—	M4.5 V	M3 V	1990 Jan 21	23
569 A	BD +16°2708	M0 V	M3 V	1989 Jul 14	20
669 A	Ross 868	M4 V	M3.5 V	1989 Jul 10	210
748 AB	Wolf 1062 AB	M4 V	M3.5 V	1989 Jul 14	30
643	Wolf 629	M4 V	M3.5 V	1989 Jul 10	1920
734 B	—	—	M3.5 V	1989 Jul 14	60
699	Barnard's Star	M5 V	M4 V	1989 Jul 10	7
232	Ross 64	M6 V	M4 V	1990 Jan 22	900
791.2	G 24-16	M6 V	M4.5 V	1989 Jul 10	210
669 B	Ross 867	M5 V	M4.5 V	1989 Jul 10	510
—	LHS 3339	—	M5.5 V	1989 Jul 13	1200
—	LHS 5142	—	M6 V	1990 Jan 21	900
—	LHS 191	—	M6.5 V	1990 Jan 21	900
—	LHS 2065	—	M9	1990 Jan 21	1500

[a] Gliese 1969 unless otherwise noted.
[b] Earlier spectral type than its companion, GL 338 A.
[c] Gliese & Jahreiss 1979.

old disk dwarfs and halo subdwarfs.) There is also a class of subdwarfs with very strong metallic hydride bands (Bessell 1982). Other stars in our survey which have been classified as subdwarfs in the past include GL 275.2 A (Eggen & Greenstein 1965), GL 213 (Joy & Abt 1974), GL 643 (Veeder 1974), and GJ 2155 (Gliese & Jahreiss 1979). In this paper, we will use the term subdwarf to refer only to those stars whose gross *spectral* characteristics distinguish them to be such. The spectrum of one such subdwarf, LHS 515, is presented here.

3. OBSERVATIONS AND DATA REDUCTION

3.1. *Dwarf Standards*

Tables 1 and 2 summarize the observations of the 77 dwarf spectral standards. All but three were observed with the Red Channel Spectrograph, equipped with a TI CCD, on the Multiple Mirror Telescope (MMT, effective aperture 4.5 m) on Mount Hopkins, Arizona. A 270 line mm^{-1} grating with an LP-495 order blocking filter was used to cover the range from 6300 to 9000 Å at a resolution of 18 Å. The remaining three dwarfs were observed on 1989 July 24 at the Steward Observatory 2.3 m telescope with the setup described in § 3.2. To assure placement of very faint objects in the aperture, we used a 2".0 wide slit. It was not deemed necessary to rotate the slit to counteract the effects of atmospheric refraction because even at an airmass of 2.00, the differential refraction between 6500 and 9000 Å is only 0".5 (Filippenko 1982). Most of these spectra were taken at airmasses of less than 1.2, where the differential refraction over this wavelength range is less than 0".2.

In the tables, GL (Gliese 1969) numbers are given in column (1) and other names are listed in column (2). Column (3) gives each object's published spectral type, and column (4) gives the spectral type determined here. The date of observa-

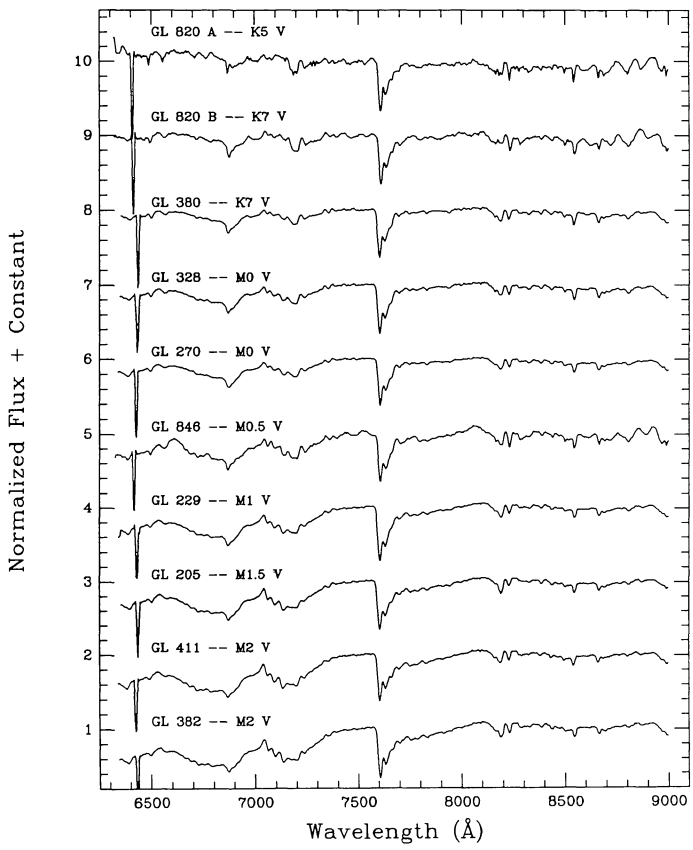

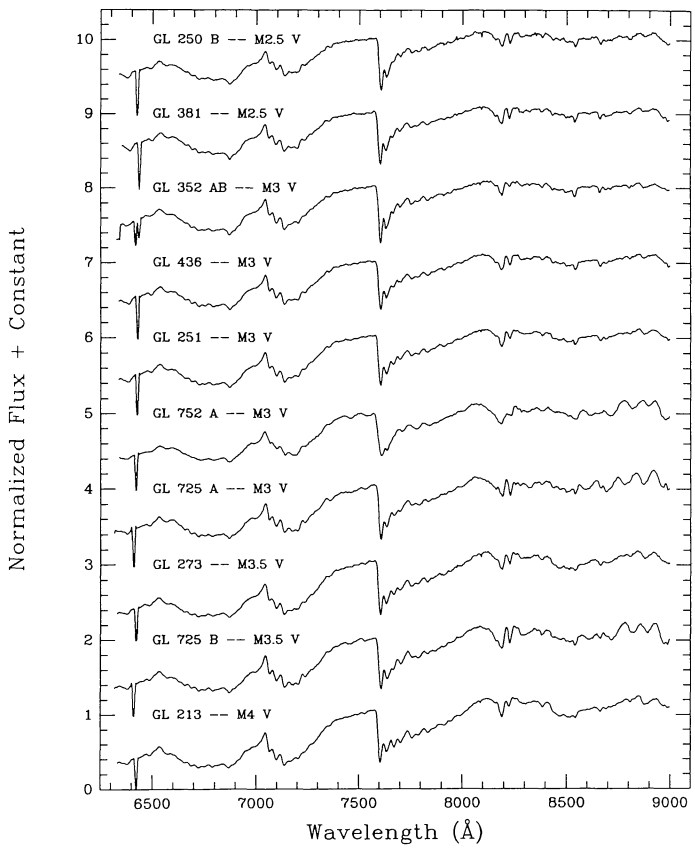

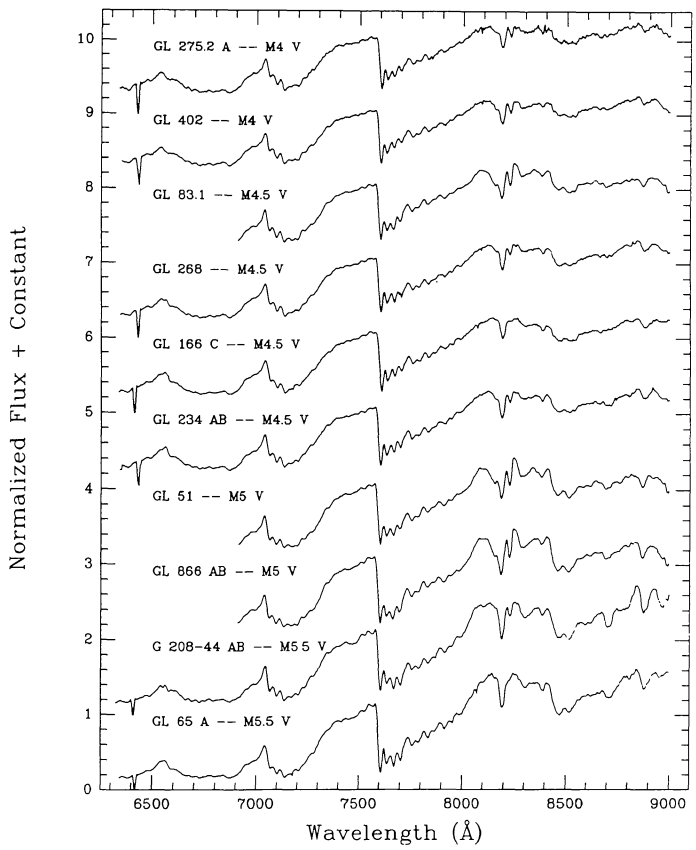

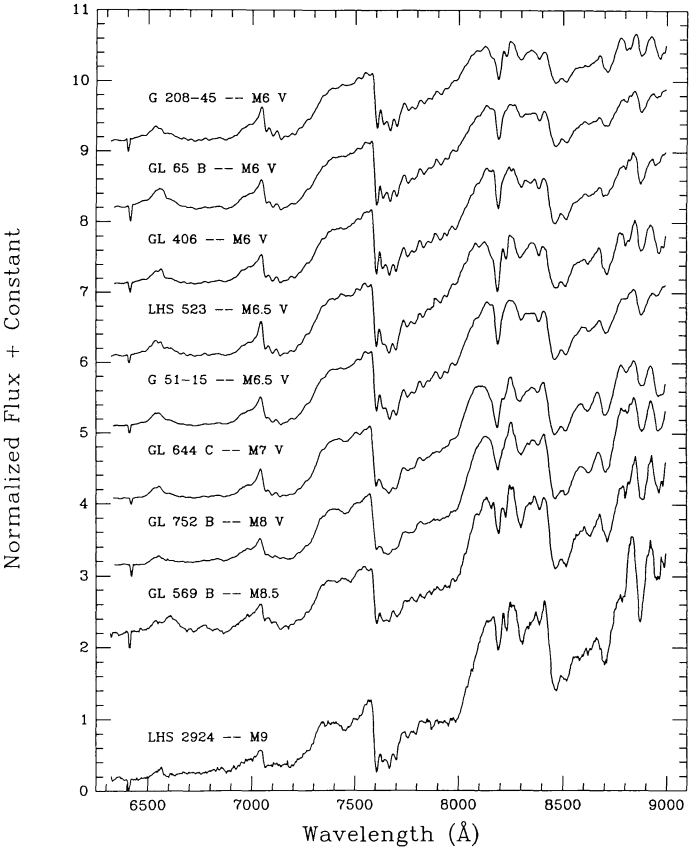

tion and the length of integration are given in columns (5) and (6).

Figures 1 and 2 show the spectra of all objects listed in Tables 1 and 2. Reduction of all spectroscopic data was done with the Image Reduction and Analysis Facility (IRAF) as follows. Each of our MMT observations was contained in a 200 × 800 pixel area on the CCD chip. To determine the bias to subtract from each row of data, we derived an estimate from 18 overscan pixels per row. The bias strip was first reduced to a one-dimensional image by medianing the pixels along rows; this value was then subtracted from the data frame, row by row. To eliminate the pixel-to-pixel variations in the dark current, a median of several dark frames was produced and then subtracted from all object, lamp, flux standard, and flat field frames. Next, to determine the pixel-to-pixel sensitivity variations over the chip, a median of the flat fields was taken and a two-dimensional surface (consisting of a low-order cubic spline along both the rows and the columns) fit to the resultant frame. This surface was then divided into each object, lamp, and standard frame.

The spectra of the program objects were not perfectly parallel to the rows of the chip. Therefore, for the sky subtraction, regions typically 7 pixels wide just above and below each object spectrum on the chip were fitted, along columns, to the background and then subtracted from each spectrum. Because the fit is done along pixel *columns* (which are not perfectly orthogonal to the dispersion axis of the sky spectrum), these areas were chosen to be close to the object spectrum so that sky subtraction would not be adversely affected. In this way, only those night sky features which are in emission have been removed; removal of absorption features such as the atmospheric A band has not been attempted.

Next, the spectra were aperture-summed to include all light from the object, and the corresponding lamps were summed over exactly the same area to preserve the wavelength information. Lines in each of the resulting one-dimensional lamp spectra (consisting of helium and argon lines) were then identified to provide a dispersion solution, which was applied to each object and standard star spectrum. Next, the spectra were extinction-corrected using the extinction coefficients for Kitt Peak, which are tabulated in IRAF, and a sensitivity function was derived for each standard spectrum. The standard stars used were from Filippenko & Greenstein (1984). Each spectrum was flux-calibrated in units of F_λ using this sensitivity function, and each was inspected for contamination by cosmic rays. Last, each spectrum was normalized to its flux at 7500 Å.

3.2. *Giant and Higher Luminosity Standards*

The giant and higher luminosity standards are given in Table 3; the description of the columns is the same as that for Tables 1 and 2, except that column (1) gives the SAO number of the star. These higher luminosity standards (with the exception of SAO 82478, which was observed with the MMT setup described above), as well as the dwarf standards GL 83.1, GL 51, and GL 866 AB, were observed with the Boller and Chivens Spectrograph with TI CCD on the Steward Observatory 2.3 m telescope on Kitt Peak, Arizona. A 400 line mm^{-1} grating was employed with a 2-59 order blocking filter to cover the spectral range from 6900 to 9000 Å. This is 600 Å less coverage than obtained at the MMT, but the resolution is improved to 8 Å. The slit width was 2″.5.

Figure 3 shows the spectra of the 14 objects listed in Table 3; the reduction was the same as for the MMT data. The flux standards were from Massey et al. (1988), where an extension, via a blackbody fit to the data, was required for wavelengths longer than 8100 Å. Each spectrum was also normalized to 7500 Å. In Figure 3 (as well as for GL 83.1, GL 51, and GL 866 AB in Fig. 1) the 2.3 m data have been rebinned and smoothed to convert them to the same resolution as the MMT data. All subsequent analyses in this paper use these rebinned and smoothed 2.3 m data.

3.3. *Miscellaneous Objects*

Table 4 gives the information on GL 756.2 and LHS 515. Both were taken with the MMT setup described above, and their spectra are shown in Figure 4. Details on these two objects are given in § 4.3.

4. SPECTRAL CLASSIFICATION

In this paper we present a different approach to spectral classification than has generally been used in the past. Instead of using only the strengths of the features to determine a spectral type, the slope of the spectrum is also used. This spectrophotometric approach is outlined in § 4.1.1 and is compared to the more widely used method in § 4.1.2.

4.1. *Primary Standards*

4.1.1. *Spectrophotometric Method*

Each of the spectra in Figure 1 was run through a least-squares minimization program to determine an ordering for the primary spectra. The program compares one normalized spectrum with each of the other normalized spectra in the list of primary standards by taking the difference between the flux values of the two spectra at 3 Å intervals in wavelength. The sum of the squares of these differences is then obtained for each pair of spectra.

The spectra have been normalized to 7500 Å because there is little absorption present at this wavelength. However, because there is some level of noise in each of the spectra, the relative normalization for any pair may not be optimal. Therefore, the

FIG. 1.—Spectra of the 39 primary dwarf standards in Table 1. All of these were observed at the MMT and have a resolution of 18 Å except for GL 83.1, GL 51, and GL 866 AB which were observed at the Steward Observatory 2.3 m telescope. These three spectra have been rebinned and smoothed so that the resolution matches that of the MMT spectra. Each of the spectra has been normalized to its flux (in units of F_λ) at 7500 Å and an offset added to separate the spectra vertically. The zero level for each spectrum is its flux value at 7500 Å (which is always an integer) minus 1. For example, the zero level for the spectrum of GL 820 A is 9. The "absorption" feature at 6415 Å is due to a dead column on the MMT CCD chip and has not been interpolated over because this is the exact location of a CaOH band. Absorption by telluric O_2 and H_2O has not been removed. GL 569 B and LHS 2924 do not have luminosity classifications given because these objects may not be true stars; they could be brown dwarfs. The same uncertain nature is true of GL 644 C (VB 8) and GL 752 B (VB 10), except that we have retained their designations of luminosity class V for historical reasons.

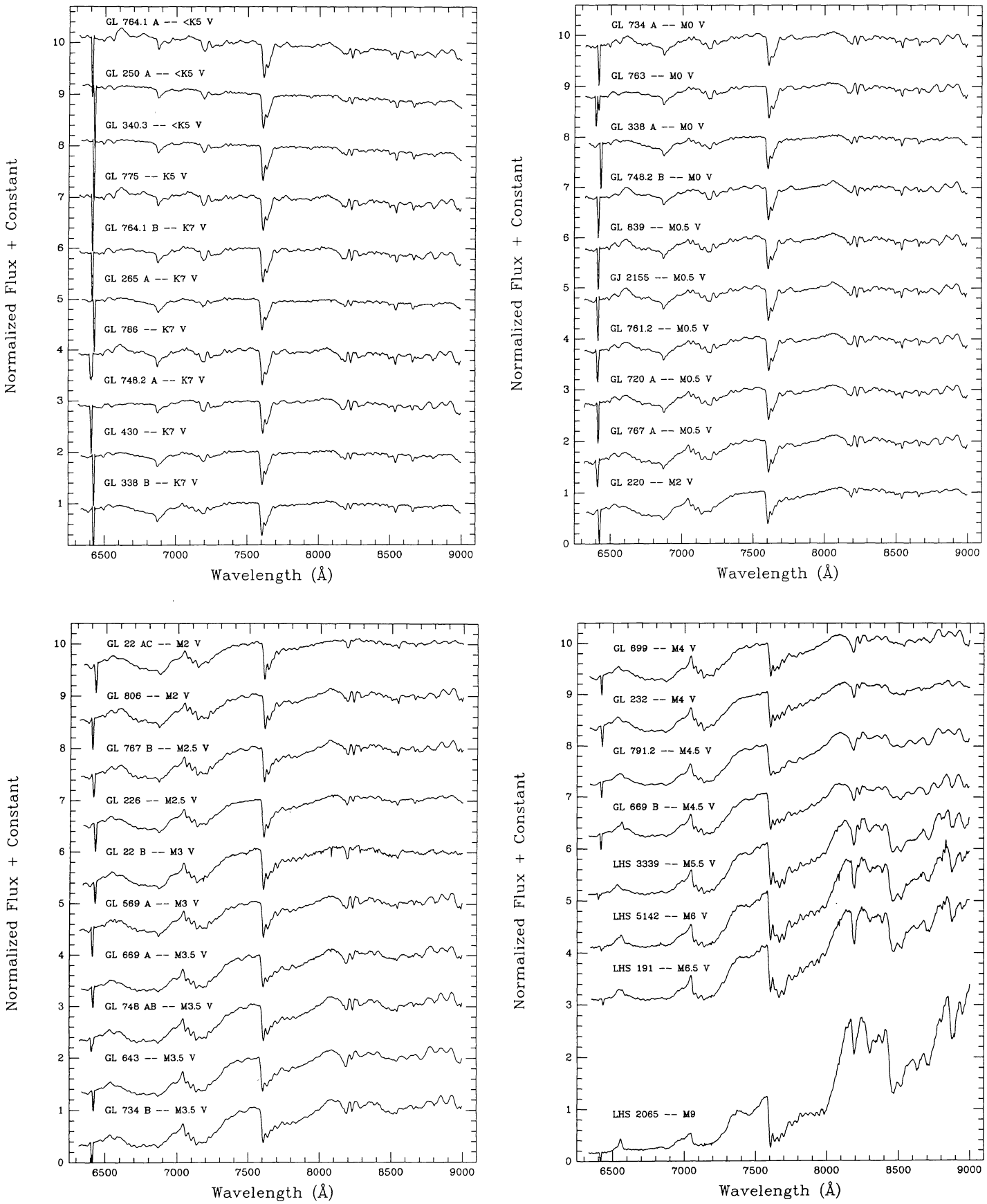

FIG. 2.—Spectra of the 38 secondary dwarf standards in Table 2. All of these were observed at the MMT and have a resolution of 18 Å. See the legend to Fig. 1 for more details.

TABLE 3

GIANT (and Higher Luminosity) SPECTRAL STANDARDS

SAO Number	Other Name	Published Spectral Type[a]	Adopted Spectral Type	Date of Observation (UT)	Integration (s)
52516	BS 8726	K5 I[b,c]	K5 I	1989 Jul 24	1
22994	HD 13136	M2 I[b]	M2 I	1989 Jul 24	15
67559	δ^2 Lyr	M4 II[d]	M4 II	1989 Jul 24	2
30653	γ Dra	K5 III[c]	K5 III	1989 Jul 24	3
21753	BD +59°128	K7 III[b]	K7 III	1989 Jul 24	50
36509	BS 152	K7 III[d,e]	K7 III	1989 Jul 24	1
141052	δ Oph	M0.5 III[d]	M0.5 III	1989 Jul 24	4
127976	55 Peg	M1 III[c]	M1 III	1989 Jul 24	4
91792	χ Peg	M2 III[f]	M2 III	1989 Jul 24	4
28843	83 UMa	M2 III[d]	M2 III	1989 Jul 24	1
63349	BD +31°2450	M3 III[b]	M3 III	1989 Jul 24	320
82478	HD 110964	M4 III[b]	M4 III	1989 Jul 10	10
34651	BS 8621	M4 III[g]	M4 III	1989 Jul 24	3
141344	HD 151061	M5 III[h]	M5 III	1989 Jul 24	4

[a] Turnshek et al. 1985 unless otherwise noted.
[b] Jacoby, Hunter, & Christian 1984.
[c] Also from Keenan & McNeil 1989.
[d] Keenan & McNeil 1976.
[e] Listed as K6 III in Keenan & McNeil 1989.
[f] Listed as M2+ III in Keenan & McNeil 1989.
[g] Listed as M4+ III in Keenan & McNeil 1989.
[h] Listed as M5 to M5.5 III in Keenan & McNeil 1989.

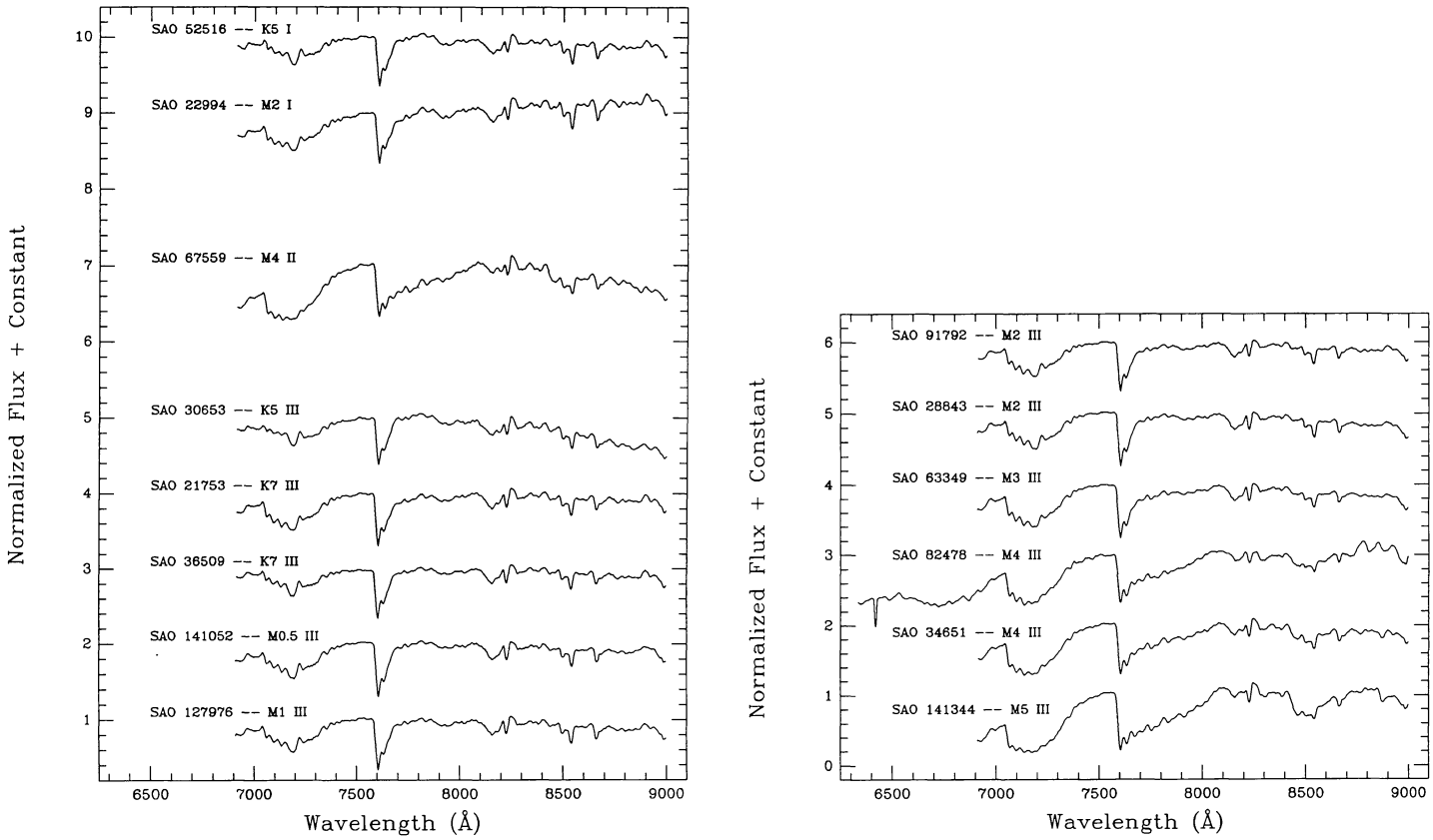

FIG. 3.—Spectra of the 14 giant and higher luminosity standards listed in Table 3. All but one of these (SAO 82478, taken at the MMT) were observed at the Steward Observatory 2.3 m telescope, but all have been rebinned and smoothed to match the resolution of the MMT spectra. See the legend to Fig. 1 for more details.

TABLE 4

MISCELLANEOUS OBJECTS

Gliese Number	Other Name	Published Spectral Type	Adopted Spectral Type	Date of Observation (UT)	Integration (s)
756.2	HD 182196	K5 V[a]	K7 III	1989 Jul 14	2
... .	LHS 515	sdMO-2[b]	sdM2.5	1989 Jul 13	1200

[a] Gliese 1969.
[b] Giampapa & Liebert 1986.

normalization for each of the spectra in the library is multiplied by a number near 1 (typically between 0.95 and 1.05) until the minimum of the squared differences between it and the spectrum being matched is found.

The minimization program can compute this "least-squares" value for any specified spectral region covered by the data. In particular, the program was used to produce least-squares matches based on the data set from 6950 to 8950 Å, on only the *short-wavelength* end of the data (6950–7500 Å), and on only the *long-wavelength* end of the data (8400–8950 Å). Wavelengths shortward of 6950 Å were not included so that the 2.3 m data, which begin around 6900 Å, could be compared to the rest of the data.

The matches on the entire data set were useful in determining a rough ordering of the spectra from bluest to reddest, but to obtain the exact ordering in those cases where two or more spectra were very similar to one another, the matches on the ends of the spectra were used. For example, consider two nearly identical spectra. If the normalization for spectrum 1 had to be multiplied by a number *greater* than 1.0 to yield the best match to spectrum 2 at the short-wavelength end, but had to be multiplied by a number *less* than 1.0 to yield the best match to spectrum 2 at the long-wavelength end, then spectrum 1 is clearly redder than spectrum 2. In this way, we ordered the entire catalog of primary standards, from bluest to reddest, and this ordering is given in Table 1.

With this ordering, the consistency between the Boeshaar (1976) spectral types and those determined here could be checked. It was found that those spectral types needing revision were changed by only a half spectral subclass at most. Of the 12 revisions, five were changed by half a subclass, and seven were changed by only a quarter of a subclass. The distinction between those with a Boeshaar designation of "plus" or "minus" and those without was not evident, so these designations were dropped from the newly adopted types. Since historically there has been little reason to introduce spectral classes K6, K8, and K9, these designations have also not been used here. In fact, it is found that in this wavelength region the differences between K5 and K7, as well as between K7 and M0, are very slight and do not warrant further subdivisions in spectral class.

For the giants, bright giants, and supergiants, the ordering technique did not result in any necessary changes in spectral class. They are listed from bluest to reddest in Table 3.

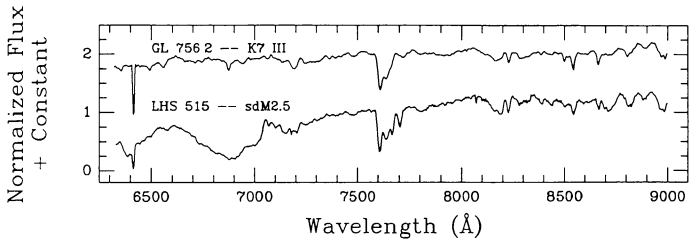

FIG. 4.—Spectra of the 2 objects listed in Table 4. Both were observed at the MMT and have a resolution of 18 Å. See the legend to Fig. 1 for more details. Note the prominent absorption lines of the Ca II triplet (8498, 8542, and 8662 Å) in the spectrum of GL 756.2 and the striking absorption feature from 6750 to 7050 Å due to CaH in the spectrum of LHS 515.

4.1.2. *"Spectral Features" Method*

The more widely used approach to spectral classification is to use the information contained in the spectral features only and to disregard the overall slope of the spectrum. To do this, the continuum must first be divided out of the data. For the latest stars, there are at best only six points in this spectral range which can possibly be labeled as continuum points: 6530, 7040, 7560, 8130, 8840, and 9040 Å. For each of the spectra in the list of primary standards, a second-order polynomial was fit to the fluxes at each of the six continuum points, and the fit was then divided out of the data to yield a flattened spectrum. The flattened spectra were then run through the least-squares minimization technique described above. In assigning an order and spectral classes to the spectra, this method and the spectrophotometric method are identical, with three minor exceptions:

1. The method using spectral features alone indicates the following ordering, from bluest to reddest, of the stars with spectral classes of M3.5 or M4: GL 725 B, GL 273, GL 402, GL 275.2 A, and GL 213. Boeshaar's original spectral classes for these are M3.5, M4, M4, M4+:, and M4+, respectively, showing no discrepancies in ordering. Our adopted spectral types for these stars are M3.5, M3.5, M4, M4, and M4, respectively, also showing no discrepancies in ordering.

2. The "spectral features" method also indicates that G208-45 and GL 65 A should be switched in the ordering of Table 1 so that the spectral class for G208-45 is identical to or earlier than GL 65 A. However, in our adopted types, as well as in the literature, G208-45 has a later spectral class than GL 65 A.

3. This second method also indicates that LHS 523 and G51-15 should be switched in the ordering of Table 1. This is of little consequence, however, because our classification, as well as that of Boeshaar, is M6.5 for both.

Therefore, the results of the two methods are almost identical. The spectrophotometric method requires that the flux calibrations for the data be relatively accurate so that any errors in the slope of the spectra remain small. The method based only on spectral features can be done without the introduction of flux calibration, but a fit to the continuum of each spectrum must be accomplished. Because the number of continuum points is small and because these are doubtless not true continuum points but rather opacity minima between certain bandheads of TiO, for example, this second method is probably more prone to error than the spectrophotometric method. Hence, the procedure outlined in § 4.1.1 will be used for spectral classification throughout the rest of this paper. It is not suggested that this method be used for more distant samples of stars since for these groups interstellar reddening could affect their classifications. The stars discussed here, however, are all nearby and therefore do not suffer from this problem.

4.2. *Secondary Standards*

Each of the secondary standards was run through the least-squares minimization program to obtain its best match in the list of primary spectra. In this way, each was assigned a spectral type. The newly adopted spectral type was often considerably different from the spectral type quoted in the literature, sometimes by as much as three subclasses. In most cases, the inconsistencies just reflect the differences between the system of Boeshaar (1976) used here and the systems quoted for their spectral types in Gliese (1969). Boeshaar's Table 3 shows several cases of spectral types disagreeing by up to two subclasses between her system and the systems of Joy & Abt (1974) and Kuiper (1938, 1942). In other cases, slight differences may be due to the fact that the current spectra are observed at longer wavelengths than have been used for spectral classification purposes previously. If a faint, unresolved, red companion is present, this may change slightly the subclass of the primary.

By the technique described in § 4.1.1, the secondary standards were also ordered from bluest and reddest. The adopted spectral types and ordering are given in Table 2. Since the secondary standards have been rigorously typed against the primary standards, both sets serve equally well as spectral standards.

4.3. *Miscellaneous Objects*

GL 756.2 was matched via least-squares minimization to the set of giant standards in Table 3 (see § 6). Its resulting spectral type is K7 III. LHS 515 was matched against the set of primary dwarf standards, but only over the region from 7050 to 8950 Å in order to exclude the CaH band from 6750 to 7050 Å. The spectrophotometric classification results in a spectral type of sdM2.5, which we have adopted in Table 4. When the "spectral features" technique is used over the same wavelength range, however, the resulting type is found to be sdM0.5, indicating that this object has weaker TiO bands, for example, than a dwarf of the same temperature.

5. LINE IDENTIFICATIONS

An extensive list of features identifiable in the spectra is given in Table 5. All obvious atomic and molecular features between 6300 and 9000 Å have been identified using sources dating back to the pioneering work of Öhman (1934). This compilation is presented here to serve as a general reference list for red/near-infrared features in late K and M stars of all luminosity classes. The question of whether each of the listed wavelengths is a laboratory value or a value measured on a spectrum was ignored because of the low resolution (18 Å) employed here. The reader, if concerned about this question, should refer to the paper(s) cited.

Figure 5 shows detailed spectra of one supergiant, three giants, three dwarfs, and one subdwarf with line identifications marked. The most obvious lines in these late-type spectra are molecular bands of TiO (and VO for the latest types) and the atomic lines of Ca II, Na I, and K I. Also obvious are the telluric lines of H_2O and the telluric A band and B band of O_2. In the cooler stars, some of the H_2O absorption is due to the stellar atmosphere, but this is generally overwhelmed by the absorption due to the earth's atmosphere (Spinrad & Newburn 1965: Spinrad et al. 1966).

As can be seen by the spectra in Figure 5, supergiants are distinguished by prominent lines of the Ca II triplet and of Fe I and Ti I, as well as prominent bands of CN. In giants of the same spectral type, all of these features are weaker. Dwarfs of similar class have even weaker lines of the Ca II triplet but have much stronger lines of the K I and Na I doublets. The one subdwarf observed shows very strong CaH bands. In short, luminosity classification of the spectra is relatively straightforward except for class II, which is virtually indistinguishable from either class I or class III in this spectral range (Keenan 1957).

As for spectral class, it is clear that K dwarfs, unlike M dwarfs, have little absorption by TiO so that their spectra have much smoother continua. The latest M dwarfs (M7 and later) are distinguished by prominent absorption by VO. Bands of CaH, which are strong in K dwarfs, disappear around spectral class M0 as TiO becomes more prominent. At the resolution of these spectra, Hα can be seen in absorption in K dwarfs and occasionally in emission in M dwarfs. Lines of Fe I and Ca II, which are strong in K through mid-M dwarfs, vanish for late-M dwarfs as absorptions by TiO and VO gain prominence.

Giants, like dwarfs, have little TiO absorption in the K-types, in contrast to mid-M types. The latest M giants are dominated by VO absorption, although none of our giant spectra are late enough to show these VO bands (Keenan & Schroeder 1952). Quantitative criteria for these classifications are given in § 6.

6. LUMINOSITY CLASSIFICATION

The least-squares minimization techniques described in § 4 are very efficient at determining spectral class, but to distinguish between luminosity classes, other criteria are needed: line ratios, flux deficits, or colors. Both line ratios and flux deficits are unsatisfactory because both of these methods require a *continuum* to be drawn to the data—a rather subjective task since M stars exhibit no true continua. Measuring colors, on the other hand, depends only upon the zero-point offset and somewhat upon the resolution of the spectrum. The zero-point dependence is minimized if we take the ratio of two colors which are closely spaced. Therefore, the emphasis here will be placed on color *ratios*.

TABLE 5

FEATURES FOUND IN LATE-K TO LATE-M SPECTRA FROM 6300 TO 9000 Å

λ (Å)	Identification	Notes	References
6322	TiO	Early to late M	1
6358			
6448			
6512			
6346	CaH	Strongest in K dwarfs	1
6382	CaH	Seen in dwarfs—disappears by mid-M; strong	2, 3, 4
6389			
6415	CaOH	(Not seen by us—it falls in the bad column on the chip)	1
6497	Ba II blended with Ti, Fe, Ca	Seen in K and early-M stars	5, 6
6563	Hα	In absorption in K stars; sometimes in emission in M stars	6
6569	TiO	Mid- to late-M stars	1
6596			
6629			
6649			
6651	TiO	Mid- to late-M stars	1
6680			
6713			
6746			
6814			
6852			
6708	Li I	Seen in some K and M stars	7, 8
6750	CaH	Strongest in early M dwarfs; particularly strong in metallic hydride subdwarfs	3, 4, 6
6903			
6908			
6921			
6946			
7050			
6867	Telluric O_2 (B band)	...	6, 7
7000			
6979	Fe I	K and early-M supergiants	6
7053	TiO	Found in all; strongest in early- to mid-M	1, 6
7087			
7124			
7159			
7197			
7219			
7270			
7186	Telluric H_2O	...	6
7273			
7334	VO	Seen only in late-M stars	6, 9
7372			
7393			
7405			
7418			
7472			
7534			
7345	Ti I	Obvious in K and early-M giants and supergiants	10
7358			
7364			
7389	Fe I	Obvious in K and early-M giants and supergiants	10
7411	Fe I	Obvious in K and early-M giants and supergiants	10
7589	TiO	Found in all; lies in atmospheric A band	11
7628			

TABLE 5—*Continued*

λ (Å)	Identification	Notes	References
7594	Telluric O_2 (A band)	...	6, 7
7685			
7665	K I	Obvious only in dwarfs and subdwarfs; blended with A band and TiO	7
7699			
7666	TiO	Prominent in M stars; strongest at mid-M	6, 12
7672			
7705			
7743			
7752			
7783			
7820			
7828			
7861			
7851	VO	Obvious in late-M dwarfs	6, 12
7865			
7897			
7900			
7919			
7929			
7939			
7961			
7967			
7973			
7878	CN	Obvious in supergiants, weaker in giants; not seen in dwarfs	11
7895			
7916			
7941			
7963			
8026			
8044			
8068			
8075	Fe I	Seen in subdwarfs	13
8164	Telluric H_2O	...	6
8177			
8183	Na I	Found in all; strongest in dwarfs	6
8195			
8206	TiO	Found in all; strongest at mid-M	6, 12
8251			
8289			
8303			
8335			
8373			
8386			
8420			
8457			
8472			
8506			
8513			
8558			
8569			
8227	Telluric H_2O	...	6
8282	Telluric H_2O	...	13
8308	Ti I and Fe I blends	Marginally visible in giants and supergiants	11
8330			
8327	Fe I	Found in K dwarfs	12, 13
8388	Fe I	Strongest in K to mid-M stars	12
8432	TiO	Prominent in mid- to late-M stars	12
8442			
8452			
8435	Ti I	Obvious in giants and supergiants	12

TABLE 5—*Continued*

λ (Å)	Identification	Notes	References
8440	Fe I	Obvious in K and early-M stars; dominated by TiO elsewhere	13
8468	Fe I, Ti I	Most obvious in giants and supergiants and K dwarfs	12, 13
8498 ..... 8542 ..... 8662	Ca II	Strongest in late-K through mid-M; strongest in supergiants then giants; weaker in dwarfs	12
8514	Fe I	Most obvious in giants and supergiants	12
8518	Ti I	Most obvious in giants and supergiants	12
8521 ..... 8538 ..... 8574 ..... 8597 ..... 8605 ..... 8624 ..... 8649 ..... 8668	VO	Found only in late-M stars	9, 12
8582 ..... 8593 ..... 8599 ..... 8611 ..... 8616 ..... 8622	Fe I	Found in K and early- to mid-M stars	13
8689	Fe I	Strongest in K dwarfs	7
8710 ..... 8713	Fe I	Strongest in K and early-M dwarfs and subdwarfs	13
8718	Mg I	Strongest in mid-M dwarfs	13
8757 ..... 8764	Fe I	Strongest in giants and supergiants	13
8793 ..... 8805	Fe I	Found in giants and supergiants	13
8807	Mg I	Found in all but late-M stars	13
8824	Fe I	Most obvious in mid-M dwarfs and subdwarfs	13
8838	Fe I	Strongest in K giants	13
8859 ..... 8868 ..... 8937	TiO	Most obvious in mid- to late-M stars	14, 15
8867	Fe I	Blended with TiO	13
8912 ..... 8924 ..... 8927	Ca II, Mg I blend	Weak in K giants	13
8952 ..... 8972	Telluric H_2O	...	13
8980 ..... 8992	Telluric H_2O	...	13

REFERENCES.—(1) Faÿ, Stein, & Warren 1974; (2) Ake & Greenstein 1980; (3) Öhman 1934; (4) Öhman 1936; (5) Gahm 1970; (6) Turnshek et al. 1985; (7) Keenan 1957; (8) Keenan & McNeil 1976; (9) Keenan & Schroeder 1952; (10) Davis 1947; (11) Sharpless 1956; (12) Solf 1978; (13) Swensson et al. 1970; (14) Wing, Spinrad, & Kuhi 1967; (15) Phillips 1950.

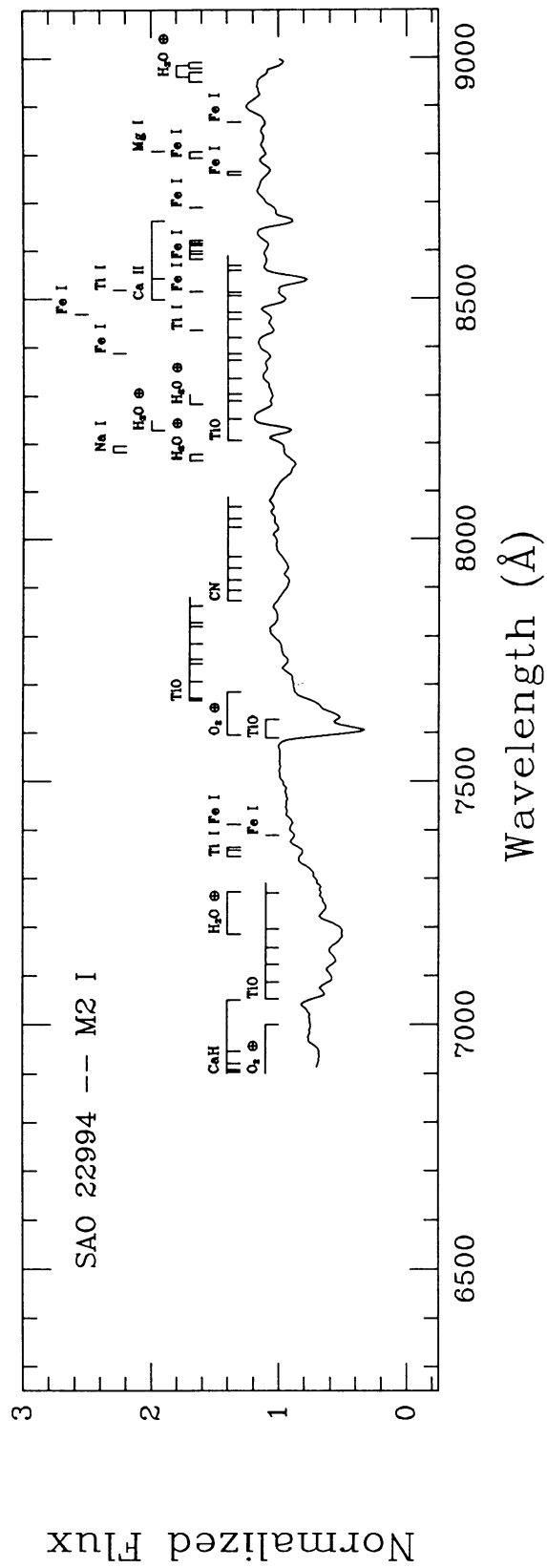

FIG. 5a

FIG. 5.—Detailed spectra of some of the objects in Figs. 1–4 with line identifications from Table 5 marked. (*a*) A supergiant of class M2. (*b*) Giants of class K5, M2, and M5. In the figure, offsets of two and four have been added to the spectra of SAO 91792 and SAO 30653, respectively, for clarity. (*c*) Dwarfs of class K5, M3.5, and M9. Offsets of four and six have been added to the spectra of GL 725 B and GL 820 A, respectively, for clarity. (*d*) A metallic hydride subdwarf of class M2.5.

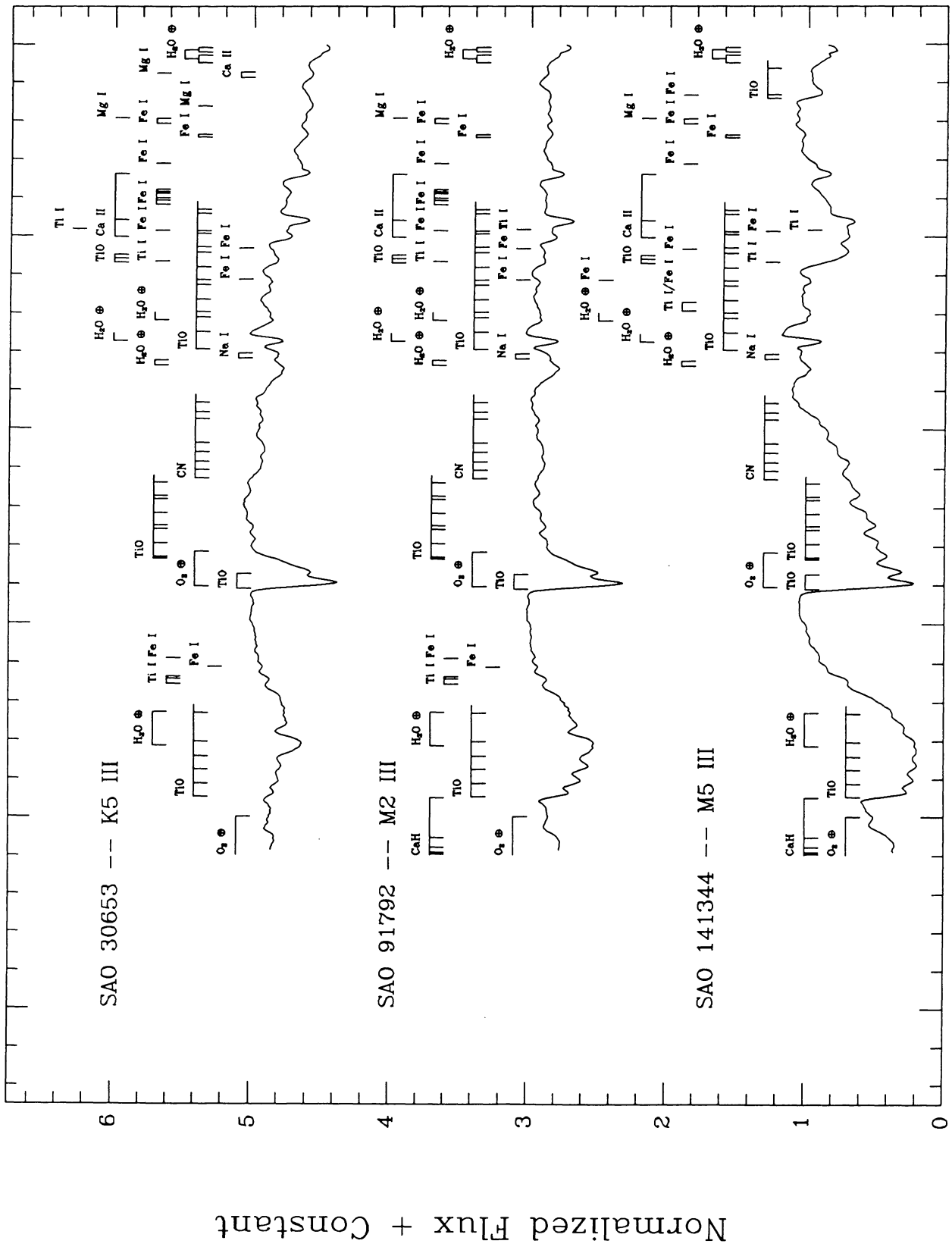

FIG. 5b

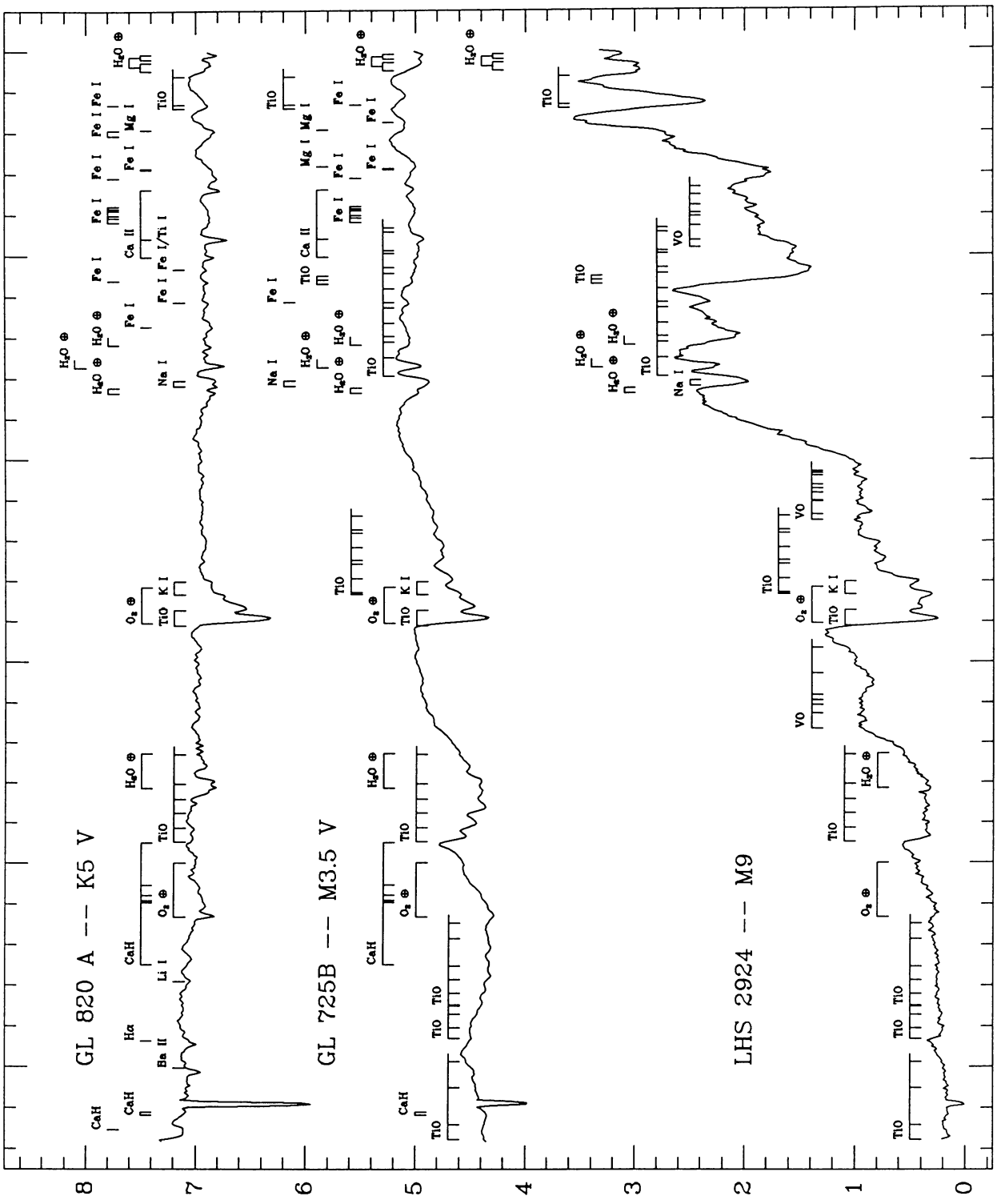

FIG. 5c

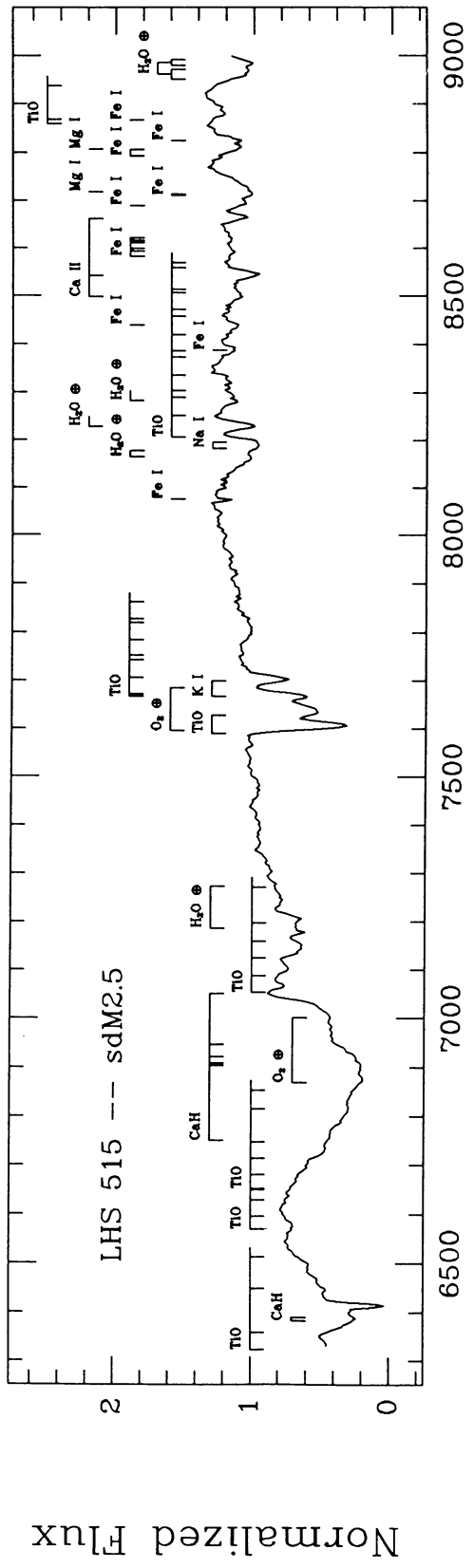

FIG. 5*d*

TABLE 6

INTEGRATION LIMITS FOR COLOR RATIOS

Ratio	Numerator	Denominator	Feature Measured
A	7020–7050 Å	6960–6990 Å	CaH λ6975
B	7375–7385 Å	7353–7363 Å	Ti I λ7358
C	8100–8130 Å	8174–8204 Å	Na I λλ8183, 8195
D	8567–8577 Å	8537–8547 Å	Ca II λλ8542

Examples of useful color ratios are shown in Figure 6. The regions over which the flux was summed were wide enough that, despite any shift due to the object's radial velocity, the features examined still fell in the flux regions. Several lines and bands given in Table 5 are useful luminosity discriminants: (*a*) the CaH band around 6975 Å is strong in metallic hydride subdwarfs, weaker in dwarfs, and even weaker in giants, (*b*) the Ti I line at 7358 Å is strongest in giants and supergiants, (*c*) the Na I doublet at 8183 and 8195 Å is strongest for the dwarfs, and (*d*) the lines of the Ca II triplet (notably the one at 8542 Å which is less contaminated by nearby lines) are strong for giants and supergiants and weak in dwarfs.

For each of the four features mentioned above, a relatively uncontaminated area in the spectrum close to the feature was found to serve as the "continuum" against which to ratio the flux. In Figure 6*a*, for example, the flux under the CaH band was integrated from 6960 to 6990 Å, and this was divided into the flux integrated in the nearby "continuum" area of the same width, from 7020 to 7050 Å. The integration limits for each of the color ratios is presented in Table 6 along with the features being measured.

All of the stars in Tables 1, 2, 3, and 4 are plotted in Figure 6 except for the three stars in Table 2 which have spectral types earlier than K5. Dwarfs are marked by filled circles, giants by open circles, the bright giant by an open square, and supergiants by crosses. The subdwarf LHS 515 is denoted by a filled square, and GL 756.2 is denoted by an open triangle. As an

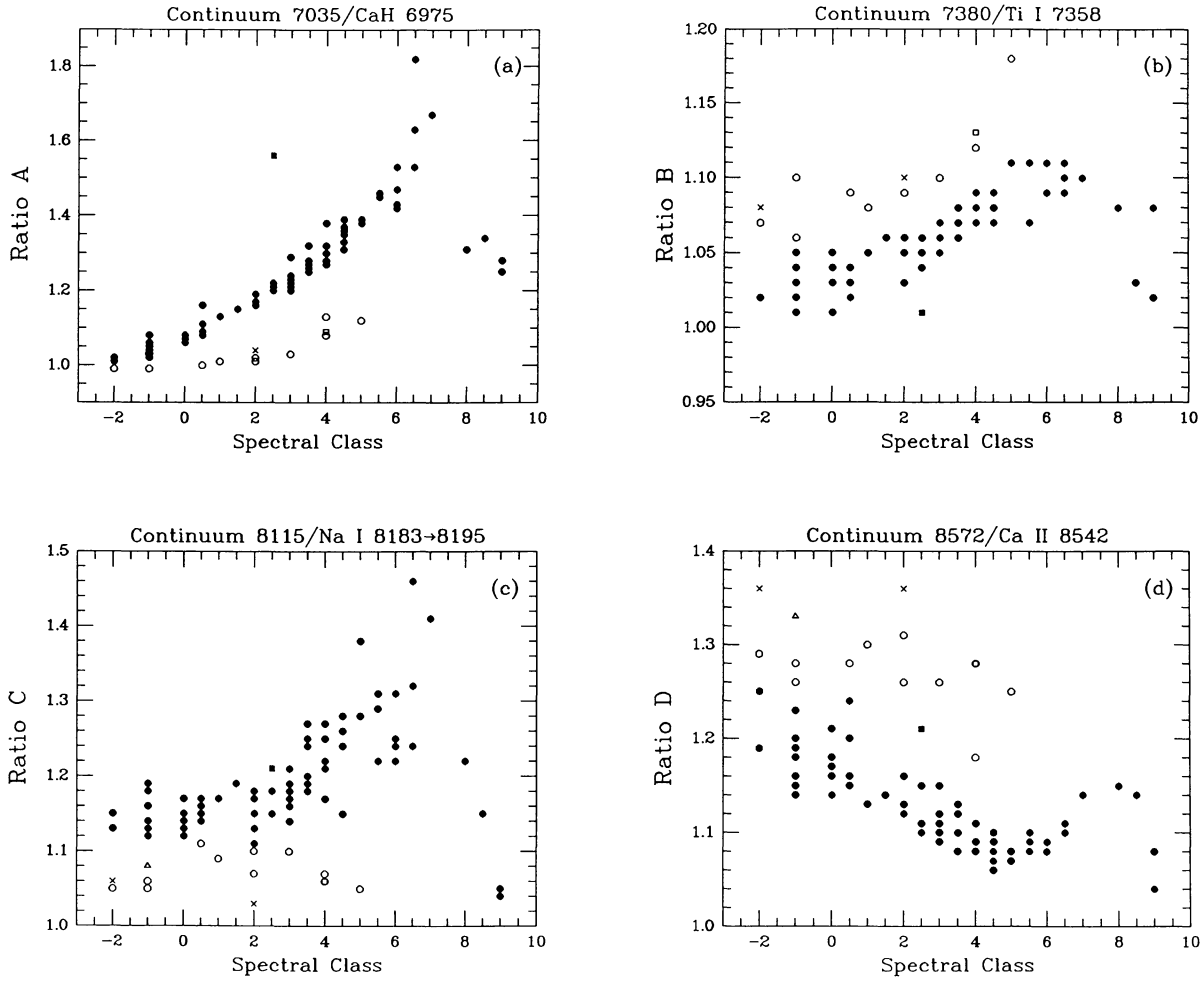

FIG. 6.—Color ratios useful as luminosity discriminants. Descriptions of the ratios are given in Table 6. Supergiants are marked by crosses, the bright giant by an open square, giants by open circles, and dwarfs by filled circles. The giant GL 756.2 is denoted by an open triangle, and the subdwarf LHS 515 is denoted by a filled square. Along the horizontal axis negative numbers represent K spectral types. K5 is located at the "−2" mark, and K7 is located at the "−1" mark. Positive numbers represent M spectral types; "0" stands for M0, "4.5" for M4.5, etc. The figure shows ratios of four different luminosity dependent lines or bands to nearby "continuum" areas, regions where there is little contaminating absorption.

example, Figure 6*a* shows that the metallic hydride subdwarf has the strongest CaH band for its spectral type, followed by the dwarfs and then the higher luminosity stars. Clearly, this criterion separates the luminosity classes very well.

In the remaining graphs of Figure 6—those involving the Ti I line, the Na I doublet, and the Ca II line—there is also a division between luminosity classes. Unfortunately, the dividing line between the dwarfs and the giants is not strong. Note, however, that for two of the graphs in Figure 6 the dwarfs fall above the giants in the diagram, and for the other two they fall below. This suggests that ratios of *these* ratios can be constructed to enhance the division between the luminosity classes. These are shown in Figure 7. Here, the separations between the dwarfs, giants, and supergiants are much more pronounced, especially in the ratios of the Ca II line at 8542 Å to the Na I doublet, shown in Figure 7*d*. Any one of the ratios shown in Figure 7 would serve as an excellent luminosity discriminant. The values of the ratios used to generate the graphs in Figures 6 and 7 are listed in Table 7.

It should be noted that GL 756.2, marked with a triangle in the figures, shows strong evidence for being a giant star and not a dwarf as published in Gliese (1969) (see Table 4). The most convincing evidence for this is shown in Figure 7*d*, where it is located well above the locus of dwarf stars but below the area occupied by the supergiants. Furthermore, its uncertain parallax is estimated spectroscopically, not trigonometrically, in the Gliese Catalog, and it has negligible proper motion. In addition, Leggett & Hawkins (1988) have noted that this star has red giant colors.

7. SPECTRAL CLASS VERSUS MASS RELATION

In an effort to provide a mass calibration for the dwarf spectral sequence established here, we have examined several M dwarfs in binary systems for which component masses have been determined dynamically (not photometrically). In practice, individual component spectra are difficult to obtain unless the two objects in the system are separated by greater than 2″. Unfortunately, such systems necessarily have long orbital periods and hence poorly determined masses. Nevertheless, five nearby M dwarfs have separations wide enough to allow the acquisition of component spectra and reasonably accurate masses: GL 65 A and B, GL 166 C, and GL 725 A and B. To this special class of objects we have added three pairs with separations less than 1″. In two of these, the primary is much more luminous than the secondary so that its light dominates

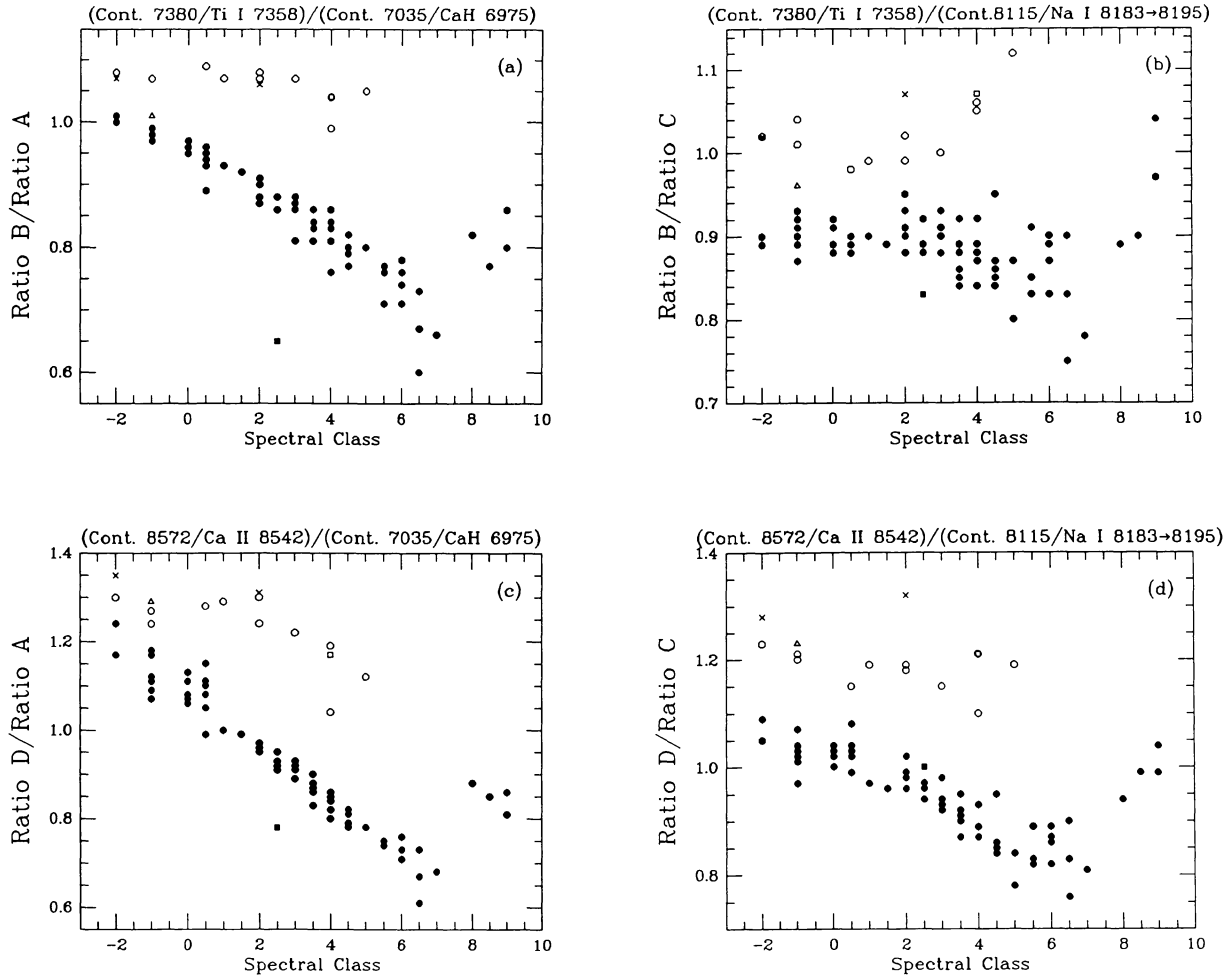

FIG. 7.—The same as Fig. 6, except that the ratios shown are based on the ratios given in Fig. 6. See text for details.

1991ApJS...77..417K

TABLE 7

COLOR RATIOS DETERMINED FROM THE SPECTRA AND PLOTTED IN FIGURES 6 AND 7

Object Name	Other Name	Adopted Spec. Type	A	B	C	D	B/A	B/C	D/A	D/C
GL 820 A	61 Cyg A	K5 V	1.02	1.02	1.13	1.19	1.00	0.90	1.17	1.05
GL 820 B	61 Cyg B	K7 V	1.02	1.01	1.12	1.20	0.99	0.90	1.18	1.07
GL 380	HD 88230	K7 V	1.06	1.04	1.16	1.18	0.98	0.90	1.11	1.02
GL 328	BD +2°2098	M0 V	1.08	1.05	1.15	1.17	0.97	0.91	1.08	1.02
GL 270	BD +33°1505	M0 V	1.08	1.04	1.14	1.14	0.96	0.91	1.06	1.00
GL 846	HD 209290	M0.5 V	1.11	1.03	1.17	1.20	0.93	0.88	1.08	1.03
GL 229	HD 42581	M1 V	1.13	1.05	1.17	1.13	0.93	0.90	1.00	0.97
GL 205	HD 36395	M1.5 V	1.15	1.06	1.19	1.14	0.92	0.89	0.99	0.96
GL 411	HD 95735	M2 V	1.17	1.05	1.13	1.12	0.90	0.93	0.96	0.99
GL 382	BD −3°2870	M2 V	1.17	1.06	1.18	1.13	0.91	0.90	0.97	0.96
GL 250 B	—	M2.5 V	1.20	1.06	1.15	1.11	0.88	0.92	0.93	0.97
GL 381	L 968-22	M2.5 V	1.22	1.05	1.18	1.11	0.86	0.89	0.91	0.94
GL 352 AB	BD −12°2918	M3 V	1.21	1.06	1.14	1.12	0.88	0.93	0.93	0.98
GL 436	BD +27°28217	M3 V	1.22	1.06	1.16	1.11	0.87	0.91	0.91	0.96
GL 251	Wolf 294	M3 V	1.24	1.07	1.18	1.10	0.86	0.91	0.89	0.93
GL 752 A	HD 180617	M3 V	1.20	1.06	1.21	1.11	0.88	0.88	0.93	0.92
GL 725 A	HD 173739	M3 V	1.23	1.06	1.17	1.09	0.86	0.91	0.89	0.93
GL 273	BD +5°1668	M3.5 V	1.25	1.08	1.18	1.08	0.86	0.92	0.86	0.92
GL 725 B	HD 173740	M3.5 V	1.28	1.07	1.24	1.13	0.84	0.86	0.88	0.91
GL 213	Ross 47	M4 V	1.28	1.08	1.17	1.09	0.84	0.92	0.85	0.93
GL 275.2 A	G 107-69	M4 V	1.30	1.08	1.22	1.09	0.83	0.89	0.84	0.89
GL 402	Wolf 358	M4 V	1.27	1.09	1.25	1.09	0.86	0.87	0.86	0.87
GL 83.1	L 1159-16	M4.5 V	1.36	1.09	1.28	1.08	0.80	0.85	0.79	0.84
GL 268	Ross 986	M4.5 V	1.31	1.08	1.24	1.06	0.82	0.87	0.81	0.85
GL 166 C	40 Eri C	M4.5 V	1.33	1.09	1.15	1.09	0.82	0.95	0.82	0.95
GL 234 AB	Ross 614 AB	M4.5 V	1.37	1.08	1.26	1.07	0.79	0.86	0.78	0.85
GL 51	Wolf 47	M5 V	1.38	1.11	1.28	1.07	0.80	0.87	0.78	0.84
GL 866 AB	L 789-6 AB	M5 V	1.39	1.11	1.38	1.08	0.80	0.80	0.78	0.78
—	G 208-44 AB	M5.5 V	1.46	1.07	1.29	1.10	0.73	0.83	0.75	0.85
GL 65 A	L 726-8	M5.5 V	1.46	1.11	1.22	1.08	0.76	0.91	0.74	0.89
—	G 208-45	M6 V	1.53	1.09	1.31	1.08	0.71	0.83	0.71	0.82
GL 65 B	UV Cet	M6 V	1.43	1.09	1.22	1.09	0.76	0.89	0.76	0.89
GL 406	Wolf 359	M6 V	1.42	1.11	1.24	1.08	0.78	0.90	0.76	0.87
—	LHS 523	M6.5 V	1.82	1.09	1.46	1.11	0.60	0.75	0.61	0.76
—	G 51-15	M6.5 V	1.53	1.11	1.24	1.11	0.73	0.90	0.73	0.90
GL 644 C	VB 8	M7 V	1.67	1.10	1.41	1.14	0.66	0.78	0.68	0.81
GL 752 B	VB 10	M8 V	1.31	1.08	1.22	1.15	0.82	0.89	0.88	0.94
GL 569 B	—	M8.5	1.34	1.03	1.15	1.14	0.77	0.90	0.85	0.99
—	LHS 2924	M9	1.28	1.02	1.05	1.04	0.80	0.97	0.81	0.99

TABLE 7—*Continued*

Object Name	Other Name	Adopted Spec. Type	A	B	C	D	B/A	B/C	D/A	D/C
GL 775	HD 190007	K5 V	1.01	1.02	1.15	1.25	1.01	0.89	1.24	1.09
GL 764.1 B	—	K7 V	1.05	1.03	1.18	1.14	0.98	0.87	1.09	0.97
GL 265 A	BD +27°1311	K7 V	1.04	1.03	1.12	1.16	0.99	0.92	1.12	1.04
GL 786	HD 193202	K7 V	1.05	1.03	1.19	1.23	0.98	0.87	1.17	1.03
GL 748.2 A	BD +1°3942	K7 V	1.04	1.02	1.14	1.15	0.98	0.89	1.11	1.01
GL 430	BD +63°965	K7 V	1.06	1.04	1.14	1.19	0.98	0.91	1.12	1.04
GL 338 B	HD 79210	K7 V	1.08	1.05	1.13	1.16	0.97	0.93	1.07	1.03
GL 734 A	HD 230017	M0 V	1.07	1.03	1.17	1.21	0.96	0.88	1.13	1.03
GL 763	HD 184489	M0 V	1.08	1.03	1.12	1.14	0.95	0.92	1.06	1.02
GL 338 A	HD 79211	M0 V	1.08	1.04	1.13	1.16	0.96	0.92	1.07	1.03
GL 748.2 B	G 22-21 B	M0 V	1.06	1.01	1.14	1.18	0.95	0.89	1.11	1.04
GL 839	G 215-20	M0.5 V	1.08	1.04	1.15	1.24	0.96	0.90	1.15	1.08
—	GJ 2155	M0.5 V	1.08	1.03	1.16	1.20	0.95	0.89	1.11	1.03
GL 761.2	BD +0°4241	M0.5 V	1.09	1.02	1.15	1.20	0.94	0.87	1.10	1.04
GL 720 A	BD +45°2743	M0.5 V	1.11	1.03	1.14	1.16	0.93	0.90	1.05	1.02
GL 767 A	BD +31°3767	M0.5 V	1.16	1.03	1.16	1.15	0.89	0.89	0.99	0.99
GL 220	Ross 59	M2 V	1.16	1.05	1.15	1.13	0.91	0.91	0.97	0.98
GL 22 AC	BD +66°34	M2 V	1.19	1.05	1.11	1.13	0.88	0.95	0.95	1.02
GL 806	G 209-41	M2 V	1.19	1.03	1.17	1.16	0.87	0.88	0.97	0.99
GL 767 B	—	M2.5 V	1.21	1.04	1.18	1.15	0.86	0.88	0.95	0.97
GL 226	AC +82°1111	M2.5 V	1.20	1.06	1.15	1.10	0.88	0.92	0.92	0.96
GL 22 B	—	M3 V	1.29	1.05	1.17	1.15	0.81	0.90	0.89	0.98
GL 569 A	BD +16°2708	M3 V	1.22	1.05	1.19	1.12	0.86	0.88	0.92	0.94
GL 669 A	Ross 868	M3.5 V	1.27	1.06	1.25	1.12	0.83	0.85	0.88	0.90
GL 748 AB	Wolf 1062 AB	M3.5 V	1.26	1.06	1.19	1.13	0.84	0.89	0.90	0.95
GL 643	Wolf 629	M3.5 V	1.32	1.07	1.27	1.10	0.81	0.84	0.83	0.87
GL 734 B	—	M3.5 V	1.26	1.06	1.20	1.10	0.84	0.88	0.87	0.92
GL 699	Barnard's Star	M4 V	1.38	1.07	1.27	1.11	0.76	0.84	0.80	0.87
GL 232	Ross 64	M4 V	1.32	1.07	1.21	1.08	0.81	0.88	0.82	0.89
GL 791.2	G 24-16	M4.5 V	1.39	1.07	1.28	1.10	0.77	0.84	0.79	0.86
GL 669 B	Ross 867	M4.5 V	1.35	1.07	1.26	1.06	0.79	0.85	0.79	0.84
—	LHS 3339	M5.5 V	1.45	1.11	1.31	1.09	0.77	0.85	0.75	0.83
—	LHS 5142	M6 V	1.47	1.09	1.25	1.08	0.74	0.87	0.73	0.86
—	LHS 191	M6.5 V	1.63	1.10	1.32	1.10	0.67	0.83	0.67	0.83
—	LHS 2065	M9	1.25	1.08	1.04	1.08	0.86	1.04	0.86	1.04

1991ApJS...77..417K

TABLE 7—*Continued*

Object Name	Other Name	Adopted Spec. Type	A	B	C	D	B/A	B/C	D/A	D/C
SAO 52516	BS 8726	K5 I	1.01	1.08	1.06	1.36	1.07	1.02	1.35	1.28
SAO 22994	HD 13136	M2 I	1.04	1.10	1.03	1.36	1.06	1.07	1.31	1.32
SAO 67559	δ^2 Lyr	M4 II	1.09	1.13	1.06	1.28	1.04	1.07	1.17	1.21
SAO 30653	γ Dra	K5 III	0.99	1.07	1.05	1.29	1.08	1.02	1.30	1.23
SAO 21753	BD +59°128	K7 III	1.03	1.10	1.06	1.28	1.07	1.04	1.24	1.21
SAO 36509	BS 152	K7 III	0.99	1.06	1.05	1.26	1.07	1.01	1.27	1.20
SAO 141052	δ Oph	M0.5 III	1.00	1.09	1.11	1.28	1.09	0.98	1.28	1.15
SAO 127976	55 Peg	M1 III	1.01	1.08	1.09	1.30	1.07	0.99	1.29	1.19
SAO 91792	χ Peg	M2 III	1.02	1.09	1.07	1.26	1.07	1.02	1.24	1.18
SAO 28843	83 UMa	M2 III	1.01	1.09	1.10	1.31	1.08	0.99	1.30	1.19
SAO 63349	BD +31°2450	M3 III	1.03	1.10	1.10	1.26	1.07	1.00	1.22	1.15
SAO 82478	HD 110964	M4 III	1.13	1.12	1.07	1.18	0.99	1.05	1.04	1.10
SAO 34651	BS 8621	M4 III	1.08	1.12	1.06	1.28	1.04	1.06	1.19	1.21
SAO 141344	HD 151061	M5 III	1.12	1.18	1.05	1.25	1.05	1.12	1.12	1.19
GL 756.2	HD 182196	K7 III	1.03	1.04	1.08	1.33	1.01	0.96	1.29	1.23
—	LHS 515	sdM2.5	1.56	1.01	1.21	1.21	0.65	0.83	0.78	1.00

TABLE 8

STARS WITH OBSERVED SPECTRA AND KNOWN MASSES

Gliese Number	Other Name	Spectral Type	Mass ($M_\odot$)	Mass Reference
22 AC[a]	BD +66°34	M2 V	0.36 ± 0.05	1
725 A	HD 173739	M3 V	0.36 ± 0.13	2
352 AB[b]	BD −12°2918	M3 V	0.22 ± 0.07	3
725 B	HD 173740	M3.5 V	0.30 ± 0.11	2
166 C	40 Eri C	M4.5 V	0.16 ± 0.03	4
.....	G 208-44 AB[a]	M5.5 V	0.12 ± 0.02	5, 6
65 A	L 726-8	M5.5 V	0.10 ± 0.01	7
65 B	UV Cet	M6 V	0.10 ± 0.01	7

[a] Primary assumed to dominate spectrum.
[b] Components assumed to be equal masses.

MASS REFERENCE.—(1) McCarthy et al. 1991; (2) Heintz 1987; (3) Heintz 1979; (4) Heintz 1974; (5) McCarthy et al. 1988; (6) Harrington 1990; (7) Geyer, Harrington, & Worley 1988.

the spectrum: for GL 22 AC, A is ~15 times brighter than C at 8000 Å; for G208-44 AB, A is ~5 times brighter than B at 8000 Å. In addition, the close binary GL 352 AB possesses components of nearly equal masses, and presumably the spectral type of both together is that of the individual stars.

Table 8 lists the masses and spectral types of the calibration M dwarfs and the references for the systems' orbital parameters. The errors given for the masses are standard errors which were determined from the literature. Shown in Figure 8 is the spectral class versus mass relation which allows mass estimates for dwarfs to be made based upon spectral class alone. Because only a few objects are available with known masses and spectra on this system, no corrections for age and metallicity effects on spectral types have been attempted.

As can be seen from Figure 8, the trend of spectral class with mass is quickly approaching the line which separates the lowest mass stars from the highest mass brown dwarfs (0.08 $M_\odot$). If the trend on this semilog plot is fit with a straight line, it is found that any object with a spectral class of approximately M7 or later can no longer be a star by virtue of its low mass. Interestingly, this is also the point in the spectral sequence where absorption by vanadium oxide becomes apparent (although at higher resolution, VO can be seen at class M5; Boeshaar 1976). However, there is no *a priori* reason to believe that the trend in Figure 8 is not, for example, asymptotic downward as the mass limit for hydrogen burning is approached. Unfortunately, we cannot presently probe any closer to the brown dwarf line because there are no reliable masses known for objects typed as M6.5 or later. All objects of extremely late spectral class are either single objects (e.g., LHS 2924 and LHS 2065) or are in binaries with very long orbital periods ($P \approx$ 500 yr for the GL 569 AB system—Forrest, Skrutskie, & Shure 1988), making accurate mass determinations impossible.

8. SUMMARY

Spectra of 93 late K to late M spectroscopic standards in the region from 6300 to 9000 Å have been presented. Spectral classification has been accomplished by using a spectrophotometric least-squares technique in which both the features and the slope of the spectrum are used. Luminosity classification has been accomplished by identifying luminosity-dependent features in the spectra and creating ratios of narrow-band colors centered on those features. An extensive list of features (from 6300 to 9000 Å) identifiable at a resolution of 18 Å in K and M stars of all luminosity classes has been produced. Using dwarfs whose masses are well determined, we have found a tight correlation of mass with spectral class which illustrates that the later M dwarfs are very quickly approaching the brown

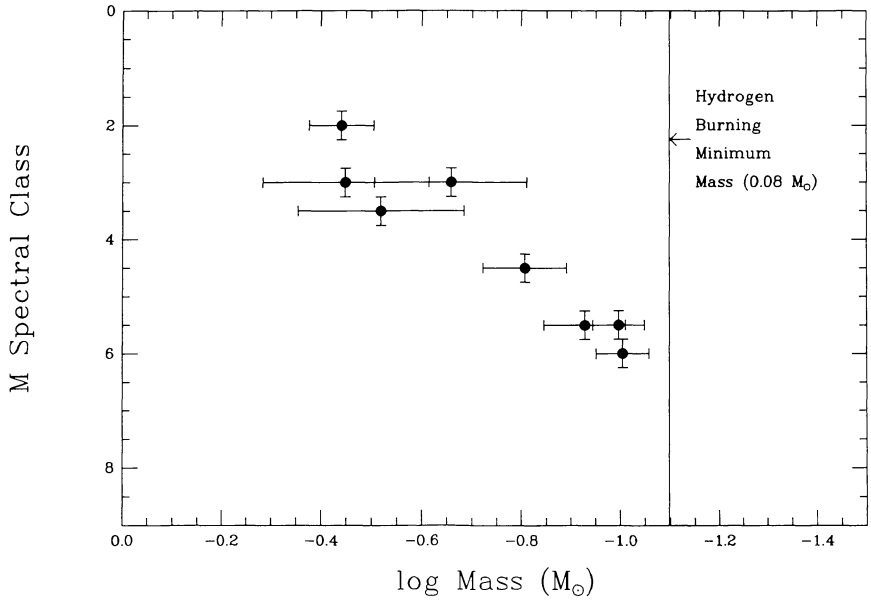

FIG. 8.—M spectral class vs. the logarithm of the mass for those dwarfs listed in Table 7. The vertical line at 0.08 $M_\odot$ represents the minimum mass for core hydrogen burning; objects to the right of the line would be brown dwarfs.

dwarf limit of 0.08 $M_\odot$. To examine the trend below 0.10 $M_\odot$ requires accurate masses to be determined for stars of class M7 or later.

The spectral sequence will also be used to check against current models of cool-star atmospheres from Allard (1990). The spectra provided here represent a stepping stone between the optical spectral sequences developed in the past and the near-infrared spectra which are rapidly approaching resolutions similar to that used for spectral classification. Eventually, moderate resolution spectra from 0.63 to 3.0 μm will be obtained for late-type stars to permit definite temperature scales to be assigned to these very red objects. It is hoped that such a calibration will allow a better determination to be made of the location of the end of the main sequence.

We would like to thank Jim Liebert and the referee, Bob Wing, for useful discussions, and we are especially indebted to Pat Boeshaar for her careful reading of the Appendix and for her many other useful comments and suggestions. We would also like to acknowledge support by the National Science Foundation through grants AST-8519506 and AST-8822465.

APPENDIX A
SPECTRAL CLASSIFICATION BEYOND M6.5

In the original MKK system of spectral classification, the dwarfs were defined only out to M2 (Morgan, Keenan, & Kellman 1943). The subsequent list of standards, the MK system (Johnson & Morgan 1953), extended the dwarf sequence out to M5 by using Barnard's Star (GL 699) as the reference standard, but this object is now sometimes classified as a subdwarf. The adoption of quantitative classification criteria for dwarfs out to M6.5 was not accomplished until the completion of Boeshaar's (1976) thesis. Before that time, M dwarfs were classified on one of three systems: the Yerkes system of Morgan (1938) and Kuiper (1942), the Mount Wilson system of Joy (1947) and Joy & Abt (1974), and various authors' attempts at extensions of the MK system.

Unfortunately, astronomers are now presented with a similar problem for spectral classification beyond M6.5. The long-known red objects VB 8 (GL 644 C) and VB 10 (GL 752 B) were not classified by Boeshaar (1976), and subsequent discoveries of objects with even cooler spectra—LHS 2924 (Probst & Liebert 1983; Liebert, Boroson, & Giampapa 1984), RG 0050-2722 (Reid & Gilmore 1981; Liebert & Ferguson 1982), LHS 2065 (Hawkins & Bessell 1988), LHS 2397a (Liebert, Boroson, & Giampapa 1984), GL 569 B (Henry & Kirkpatrick 1990), ESO 207-61 (Ruiz, Takamiya, & Roth 1991), and LHS 3002 (Bessell 1991), as well as CTI 115638.5+280002 and CTI 012657.5+280202 (Kirkpatrick 1991)—prompted another extension of the classification system. Liebert was the first to obtain spectra of many of these late objects, and Boeshaar was asked for her input in assigning their spectral types. These later types, which are presented in Boeshaar & Tyson (1985), have been used throughout this paper as the basis for the classification of the reddest objects.

In the meantime, Wing was continuing to develop a classification system based on narrow-band photometry of TiO bands. Between M0 and M6, Wing's spectral types are almost identical to those of Boeshaar (Wing & Yorka 1979), but later than this the two systems rapidly diverge. In his system, dwarfs and giants of the same spectral subclass have the same TiO band strengths (Wing 1979). Bessell (1991) has adopted Wing's system and assigns types as late as M10 for giants and as late as M7 for dwarfs. For the coolest dwarfs, he also uses the appearance of VO as an indicator of type, doubtless out of necessity because the TiO bands saturate. A comparison between the latest types used in this paper and those adopted by Bessell (1991) is shown in Table 9.

TABLE 9

SPECTRAL TYPES FOR THE COOLEST "DWARFS"

NAME	SPECTRAL TYPES[a]	
	This Paper	Bessell 1991
GL 644 C (VB 8)	M7	M6.5
CTI 115638.5+280002	M7[b]	...
LHS3002[c]	...	M7
GL 752 B (VB 10)	M8	M7
LHS 2397a	M8[b]	M7
GL 569 B	M8.5	...
CTI 012657.5+280202	M8.5[b]	...
LHS 2065	M9	M7
LHS 2924	M9	M7

[a] Spectral types have not yet been obtained on either system for the very red objects RG 0050–2722 and ESO 207–61, the first of which is classified as M8 by Boeshaar 1991.

[b] Spectral types from Kirkpatrick 1991.

[c] Classified as M7 by Boeshaar 1991.

Our reasons for adopting the spectral type extension out to M9 are as follows:

1. Morgan states that the standards of reference for the MK system "do not depend on values of any specific line intensities or ratio of intensities; they have come to be defined by the appearance of the totality of lines, blends, and bands in the ordinary photographic region" (Morgan & Keenan 1973). Bessell (1991) objects to the use of even the "yellow" portion of the spectrum for late M classification and endorses the use of temperature sensitive features in a region near the maximum flux—a valid point which is the reason that his spectra and those of this paper cover nearly the same spectral region. Using TiO band strengths as the sole indicator of spectral type, however, is undesirable because it disregards all of the other information present in the spectrum (the totality of which Morgan speaks). Furthermore, Bessell (1991) determines the TiO band strengths by fitting a blackbody curve through the highest "continuum" points. Allard (1990) has calculated M dwarf atmospheres before and after the addition of TiO, H_2O, and atomic lines. The depression of the entire spectrum after the addition of these atoms and molecules is striking. Thus, the highest points in an M dwarf spectrum are much below the location of the true continuum, making absolute band strengths unreliable. Ratios are better, and the use of many temperature sensitive ratios is the best.

2. Note that all of the objects in Table 9 have the same Bessell type (M7) except for VB 8 (GL 644 C), which is half a spectral subclass earlier. For the same objects, the classifications in this paper range from M7 to M9. Adopting a system which extends to M9 satisfies the basic tenet which underlies any classification system in any science—things which appear different should be placed into separate categories. The subtle differences in spectral features which distinguish an M0 dwarf from an M1 dwarf may not be immediately apparent from the spectra of Figure 1, but the differences between M7 and M8, or between M8 and M9, are obvious. If spectra which look very similar (like M0 and M1) are segregated, then spectra like those of M7, M8, and M9 should not be placed into the same subclass.

3. A very fundamental reason for having several subclasses for the coolest spectra, even if few of these objects are currently known, is to search for any peculiarities which could distinguish the spectrum of a brown dwarf from that of a low-mass star. Above all else, it is these differences that should be noted.

REFERENCES

Abt, H. A. 1963, ApJS, 8, 99
Ake, T. B., & Greenstein, J. L. 1980, ApJ, 240, 859
Allard, F. 1990, Ph.D. thesis, Univ. Heidelberg
Berriman, G., & Reid, N. 1987, MNRAS, 227, 315
Bessell, M. S. 1982, Proc. ASA, 4, 417
———. 1991, AJ, 101, 662
Boeshaar, P. C. 1976, Ph.D. thesis, Ohio State Univ.
———. 1991, private communication
Boeshaar, P. C., & Tyson, J. A. 1985, AJ, 90, 817
Davis, D. N. 1947, ApJ, 106, 28
Eggen, O. J., & Greenstein, J. L. 1965, ApJ, 141, 83
Faÿ, T. D., Jr., Stein, W. L., & Warren, W. H., Jr. 1974, PASP, 86, 772
Filippenko, A. V. 1982, PASP, 94, 715
Filippenko, A. V., & Greenstein, J. L. 1984, PASP, 96, 530
Forrest, W. J., Skrutskie, M. F., & Shure, M. 1988, ApJ, 330, L119
Gahm, G. F. 1970, A&A, 4, 268
Geyer, D. W., Harrington, R. S., & Worley, C. E. 1988, AJ, 95, 1841
Giampapa, M. S., & Liebert, J. 1986, ApJ, 305, 784
Gliese, W. 1969, Veroff. Astr. Rechen-Inst. Heidelberg, No. 22
Gliese, W., & Jahreiss, H. 1979, A&AS, 38, 423
Harrington, R. S. 1990, AJ, 100, 559
Hawkins, M. R. S., & Bessell, M. S. 1988, MNRAS, 234, 177
Heintz, W. D. 1974, AJ, 79, 819
———. 1979, AJ, 84, 1223
———. 1987, PASP, 99, 1084
Henry, T. J., & Kirkpatrick, J. D. 1990, ApJ, 354, L29
Jacoby, G. H., Hunter, D. A., & Christian, C. A. 1984, ApJS, 56, 257
Johnson, H. L., & Morgan, W. W. 1953, ApJ, 117, 313
Joy, A. H. 1947, ApJ, 105, 96
Joy, A. H., & Abt, H. A. 1974, ApJS, 28, 1
Keenan, P. C. 1957, PASP, 69, 5
Keenan, P. C., & McNeil, R. C. 1976, An Atlas of Spectra of the Cooler Stars: Types G, K, M, S, and C (Columbus: Ohio State Univ. Press)
———. 1989, ApJS, 71, 245
Keenan, P. C., & Schroeder, C. W. 1952, ApJ, 115, 82
Kirkpatrick, J. D. 1991, in preparation
Kuiper, G. P. 1938, ApJ, 87, 592
———. 1942, ApJ, 95, 201
Leggett, S. K., & Hawkins, M. R. S. 1988, MNRAS, 234, 1065
Liebert, J., Boroson, T. A., & Giampapa, M. S. 1984, ApJ, 282, 758
Liebert, J., & Ferguson, D. H. 1982, MNRAS, 199, 29P
Luyten, W. J. 1979, The LHS Catalogue (2d ed.; Minneapolis: Univ. of Minnesota Press)
Massey, P., Strobel, K., Barnes, J. V., & Anderson, E. 1988, ApJ, 328, 315
McCarthy, D. W., Jr., Henry, T. J., Fleming, T. A., Saffer, R. A., Liebert, J., & Christou, J. C. 1988, ApJ, 333, 943
McCarthy, D. W., Jr., Henry, T. J., McLeod, B. A., & Christou, J. C. 1991, AJ, 101, 214
Merrill, P. W., Deutsch, A. J., & Keenan, P. C. 1962, ApJ, 136, 21
Morgan, W. W. 1938, ApJ, 87, 589
Morgan, W. W., & Keenan, P. C. 1973, ARA&A, 11, 29
Morgan, W. W., Keenan, P. C., & Kellman, E. 1943, An Atlas of Stellar Spectra (Chicago: Univ. of Chicago Press)
Mould, J. R. 1976, ApJ, 207, 535
Mould, J. R., & McElroy, D. B. 1978, ApJ, 220, 935
Öhman, Y. 1934, ApJ, 80, 171
———. 1936, Stockholms Obs. Ann., 12, No. 3
Phillips, J. G. 1950, ApJ, 111, 314
Probst, R. G., & Liebert, J. 1983, ApJ, 274, 245
Reid, I. N., & Gilmore, G. 1981, MNRAS, 196, 15P
Ruiz, M. T., Takamiya, M. Y., & Roth, M. 1991, ApJ, 367, L59
Sharpless, S. 1956, ApJ, 124, 342
Solf, J. 1978, A&AS, 34, 409
Spinrad, H., & Newburn, R. L., Jr. 1965, ApJ, 141, 965
Spinrad, H., Pyper, D. M., Newburn, R. L., Jr., & Younkin, R. L. 1966, ApJ, 143, 291
Swensson, J. W., Benedict, W. S., Delbouille, L., & Roland, G. 1970, The Solar Spectrum from λ7498 to λ12016: A Table of Measures and Identifications (Liège: Institute D'Astrophysique de L'Université de Liège)
Turnshek, D. E., Turnshek, D. A., Craine, E. R., & Boeshaar, P. C. 1985, An Atlas of Digital Spectra of Cool Stars (Tucson: Western Research Co.)
Veeder, G. J. 1974, AJ, 79, 1056
Wing, R. F. 1979, in IAU Colloquium 47, Spectral Classification of the Future, ed. M. F. McCarthy, A. G. D. Philip, & G. V. Coyne (Vatican City: Vatican Observatory), 347
Wing, R. F., Spinrad, H., & Kuhi, L. V. 1967, ApJ, 147, 117
Wing, R. F., & Yorka, S. B. 1979, in IAU Colloquium 47, Spectral Classification of the Future, ed. M. F. McCarthy, A. G. D. Philip, & G. V. Coyne (Vatican City: Vatican Observatory), 519